

**DEVELOPMENT OF A
GREEN SELF-POWERED SENSOR**

WAYNE LIM YIN HERN

UNIVERSITI TUNKU ABDUL RAHMAN

DEVELOPMENT OF A GREEN SELF-POWERED SENSOR

WAYNE LIM YIN HERN


**A project report submitted in partial fulfilment of the
requirements for the award of Bachelor of Mechatronics
Engineering with Honours**

**Lee Kong Chian Faculty of Engineering and Science
Universiti Tunku Abdul Rahman**

October 2024

DECLARATION

I hereby declare that this project report is based on my original work except for citations and quotations which have been duly acknowledged. I also declare that it has not been previously and concurrently submitted for any other degree or award at UTAR or other institutions.

Signature : 

Name : WAYNE LIM YIN HERN

ID No. : 2200436

Date : 3 October 2024

APPROVAL FOR SUBMISSION

I certify that this project report entitled “**DEVELOPMENT OF A GREEN SELF-POWERED SENSOR**” was prepared by **WAYNE LIM YIN HERN** has met the required standard for submission in partial fulfilment of the requirements for the award of Bachelor of Mechatronics Engineering with Honours at Universiti Tunku Abdul Rahman.

Approved by,

Signature

:



Supervisor

:

Dr. Low Jen Hahn

Date

:

3/10/2024

The copyright of this report belongs to the author under the terms of the copyright Act 1987 as qualified by Intellectual Property Policy of Universiti Tunku Abdul Rahman. Due acknowledgement shall always be made of the use of any material contained in, or derived from, this report.

© 2024, WAYNE LIM YIN HERN. All right reserved.

ACKNOWLEDGEMENTS

I would like to thank everyone who had contributed to the successful completion of this project. I would like to express my gratitude to my research supervisor, Dr. Low Jen Hahn for his invaluable advice, guidance and his enormous patience throughout the development of the research.

In addition, I would also like to express my gratitude to my loving parents and friends who had helped and given me encouragement to complete my final year project when I faced many obstacles.

ABSTRACT

The rapid expansion of the Internet of Things (IoT) has fueled a growing demand for high-performance sensors that are not only efficient but also sustainable. This demand has accelerated the development of sensors that are compact, lightweight, and environmentally friendly. Traditional sensors, which are typically rigid and reliant on bulky power sources, no longer meet the needs of modern, sustainable technologies. Simultaneously, there has been a significant shift toward renewable energy and energy harvesting technologies. In this context, this project explores the use of Triboelectric Nanogenerators (TENG) as a cutting-edge solution to replace conventional sensors. TENGs leverage the triboelectric effect to convert mechanical energy into electrical energy, enabling them to operate as self-powered sensors. The device functions through the contact separation mechanism between two materials— polyvinyl chloride (PVC) and paper—producing a potential difference that serves as the electrical signal. This approach eliminates the need for external power sources, aligning with the principles of sustainability and energy efficiency. Moreover, the project emphasizes the use of green materials, designing the sensor for reuse, easy disassembly, and remanufacturing. Recyclable materials are prioritized, with Arabic gum-graphite composite being utilized as a key component for the electrode due to its rewettable and reusable properties, allowing it to be shaped and reshaped as needed. The fabricated sensor is then applied in a human-machine interface (HMI) context, specifically in controlling the movement of a paddle in a ping-pong game. The sensor enables precise control, allowing the paddle to move left and right, while the game score is displayed in real-time on the Blynk IoT platform. This integration of a self-powered sensor into an IoT application demonstrates the potential of TENG technology in creating sustainable, high-performance systems that meet the evolving needs of IoT-driven innovations.

TABLE OF CONTENTS

DECLARATION		i
APPROVAL FOR SUBMISSION		ii
ACKNOWLEDGEMENTS		iv
ABSTRACT		v
TABLE OF CONTENTS		vi
LIST OF TABLES		viii
LIST OF FIGURES		ix
LIST OF SYMBOLS / ABBREVIATIONS		xi
LIST OF APPENDICES		xiii
CHAPTER		
1	INTRODUCTION	1
1.1	Background of Energy Harvesting and Green Product Material	1
1.2	Importance of the Study	2
1.3	Problem Statement	2
1.4	Aim and Objectives	3
1.5	Scope and Limitation of the Study	3
1.6	Contribution of the Study	4
1.7	Outline of the Report	4
2	LITERATURE REVIEW	6
2.1	Introduction	6
2.2	Self-powered Mechanisms	6
2.2.1	Photovoltaic	6
2.2.2	Electromagnetic Generator	7
2.2.3	Biofuel Cells	8
2.2.4	Radio-frequency	9
2.2.5	Thermoelectric Generator	10
2.2.6	Piezoelectric Nanogenerator	11

2.3	Triboelectric Nanogenerators	12
2.3.1	Four Working Modes for Triboelectric Nanogenerators	12
2.3.2	Triboelectric Series	14
2.3.3	Green Dielectric Material	15
2.3.4	Green Electrode Material	18
2.4	Summary	21
3	METHODOLOGY AND WORK PLAN	22
3.1	Introduction	22
3.2	Fabrication of Self-powered Sensor	22
3.2.1	Dielectric Material	22
3.2.2	Preparation of Arabic Gum-Graphite Composite Electrode	23
3.3	Fabrication Process of Green Self-powered Sensor	26
3.4	Characterization of the Self-powered Sensor	27
3.5	Internet of Things	29
3.6	Gantt Chart	30
3.7	Summary	31
4	RESULTS AND DISCUSSION	32
4.1	Introduction	32
4.2	Mechanical and Electrical Properties of Electrode	32
4.3	Characterization of Green Self-powered Sensor	35
4.4	Durability Test	39
4.5	IOT Self-Powered Sensor Application	40
4.6	Summary	42
5	CONCLUSIONS AND RECOMMENDATIONS	44
5.1	Conclusions	44
5.2	Recommendations for Future Work	44
	REFERENCES	46
	APPENDICES	48

LIST OF TABLES

Table 2.1:	Green Materials from Empirical Triboelectric Series.	15
Table 3.1:	FYP1 Gantt Chart	30
Table 3.2:	FYP2 Gantt Chart	31

LIST OF FIGURES

Figure 2.1:	Principle of PV self-powered technologies. Reprinted with permission from copyright 2022 Elsevier.	7
Figure 2.2:	Practical of the water-proof hybrid generator. Reprinted with permission from copyright 2015 Advanced Energy Materials.	8
Figure 2.3:	Anode and cathode pastes that are completely edible are contained inside a hollow almond to form an implantable ethanol biofuel cell. Reprinted with permission from copyright 2024 ASC Biomaterials Science & Engineering.	9
Figure 2.4:	(a) Matching network with 50 Ω antenna and (b) matched single-ended loop antenna. Reprinted with permission from copyright 2023 IEEE.	10
Figure 2.5:	Design of CNT/PLA TE composite fabric and its function in wearable TE generators and temperature sensing. Reprinted with permission from copyright 2023 Composites Science and Technology.	11
Figure 2.6:	Digital image of the foot stamp at different stages. Reprinted with permission from copyright 2015 Elsevier.	12
Figure 2.7:	(a) Vertical contact separation mode, (b) sliding mode, (c) single electrode mode, and (d) free-standing mode. Reprinted with permission from copyright 2022 Joule.	13
Figure 2.8:	Empirical Triboelectric Series. Reprinted with permission from copyright 2022 Joule.	14
Figure 2.9:	Production method of PLA and gelatin plates. Reprinted with permission from copyright 2018 Elsevier.	16
Figure 2.10:	Photos of the disintegrating PLA/Mg sheets, Mg foil, and gelatine/Mg in natural water. Reprinted with permission from copyright 2018 Elsevier.	17
Figure 2.11:	Fabrication process of bamboo leaf and polytetrafluoroethylene (PTFE) film. Reprinted with permission from copyright 2024 MDPI.	17
Figure 2.12:	Simple circuit conductive dough with LED. Reprinted with permission from copyright 2018 Springer Nature.	18

Figure 2.13:	Fabrication for WCG - derived TENG. Reprinted with permission from copyright 2022 Global Challenges.	20
Figure 3.1:	The triboelectric series includes paper, cotton, and PVC.	23
Figure 3.2:	Electrode bending test.	24
Figure 3.3:	Arabic gum-graphite composite and copper sheet samples on SEM sample holder.	26
Figure 3.4:	Fabrication process.	27
Figure 3.5:	Digital multimeter.	28
Figure 3.6:	Machine tapping test.	29
Figure 3.7:	Circuit diagram for ping pong game.	30
Figure 4.1:	Young's Modulus of Arabic gum-graphite composite.	33
Figure 4.2:	Electrical conductivity of Arabic gum-graphite composite.	34
Figure 4.3:	SEM of Arabic gum-graphite composite and copper.	35
Figure 4.4:	Prototype of self-powered sensors (1) PVC/cloth-copper, (2) PVC/paper-copper, and (3) PVC/paper-Arabic gum-graphite composite.	36
Figure 4.5:	Potential differences are generated based on the types of materials used.	36
Figure 4.6:	Sensor output from a single contact and separation event using PVC/Paper-Arabic gum-graphite (5:10).	37
Figure 4.7:	Working principle of contact separation mode.	38
Figure 4.8:	Output of the self-powered sensor with varying applied forces.	38
Figure 4.9:	Output of the self-powered sensor with varying applied displacement.	39
Figure 4.10:	Output of PVC/paper-Arabic gum-graphite composite using self-powered sensor over 1000 cycles.	40
Figure 4.11:	Ping pong game controlled by self-powered sensor.	41
Figure 4.12:	Ping pong game controlled by self-powered sensor.	41
Figure 4.13:	Blynk IOT dashboard with 2 scores.	42

LIST OF SYMBOLS / ABBREVIATIONS

I	moment of inertia, m ³
b	width, m
h	thickness, m
δ	deflection, m
F	force, N
L	length, m
E	young's modulus, GPa
σ	electrical conductivity
R	resistance, ohm
l	distance between the probes, cm
A	cross-sectional area, cm ²
AC	Alternating current
BD-TENGs	Biodegradable triboelectric nanogenerators
DTNG	Droplet-based triboelectric nanogenerator
EMGs	Electromagnetic Generators
FYP	Final Year Project
HMI	Human-machine interface
IoT	Internet of Things
Mg	Magnesium
OLED	Organic Light Emitting Diode
PDMS	Polydimethylsiloxane
PENG	Piezoelectric nanogenerator
PLA	Polylactic acid
PV	Photovoltaic
PTFE	Polytetrafluoroethylene
PVC	Polyvinyl chloride
RC	Resistive-capacitive
RF	Radio-frequency
SEM	Scanning Electron Microscope
TE	Thermoelectric

TENG	Triboelectric nanogenerators
WPHG	Water-Proof Triboelectric-Electromagnetic Hybrid Generator
WCG	Waste coffee grounds

LIST OF APPENDICES

Appendix A: Supporting Graphs for the Durability Test	48
Appendix B: Supporting Attachments for Ping Pong Ball Application	50
Appendix C: Open Access to Image Rights	56

CHAPTER 1

INTRODUCTION

1.1 Background of Energy Harvesting and Green Product Material

The new way of connecting objects or Things with the ability to understand and analyze information is called the Internet of Things (IoT). It's like a big step forward in how factories and machines work. It uses a bunch of cool stuff like tiny sensors, wireless communication, and smart energy use. IoT is the leader of this big change in technology, which some people call the Third Industrial Revolution (Syeda Adila et al., 2018). Creating sensors that can power themselves will collect information about how humans move. This is useful for things like recognizing how people move and how they interact with machines, which are all connected to the Internet of Things (IoT). When it comes to products used by people, making sure they work well, feel comfortable, and are safe is really important. That's why sensors play a big part in gathering information about how people move and behave.

According to Lai et al. (2022), the rise of energy harvesters that rely on human motion signals a growing necessity for creating sustainable energy sources for small devices powered by human movement. Various energy conversion methods are explored, such as electromagnetic, piezoelectric, and triboelectric nanogenerator mechanisms, among others. These energy sources find applications across diverse fields, ranging from large-scale industries like manufacturing, engineering, agriculture, and transportation to powering smaller-scale devices like lighting, entertainment gadgets, low-power electronics, and wearable technology.

Based on Dangelico & Pontrandolfo (2010), a green product is one that minimizes its environmental impact through sustainable practices. This involves using fewer materials than traditional alternatives to reduce the negative effects on the environment. These products may be made from recycled or natural, biodegradable materials at sustainable rates, leading to minimal environmental impact. They are also often designed for reuse, easy disassembly, and remanufacturing, or made from recyclable materials. This approach not only boosts their sustainability but also reduces the need for new

materials, thereby lessening the environmental impact of their production. In a nutshell, this project will create an IoT-integrated, self-powered sensor utilizing green materials.

1.2 Importance of the Study

The importance of nanogenerators lies in their revolutionary potential to capture environmental mechanical power and then convert it into electrical power thereby paving the way for self-sustaining and renewable energy solutions. Nanogenerators provide a potential alternative to conventional energy sources for small-scale electronic device powering. Their compact size, scalability, and ability to operate in diverse environments make them invaluable for various applications, for example implantable medical devices to sensor networks and Internet of Things (IoT) systems. Furthermore, nanogenerators hold significant promise for powering remote or inaccessible locations where conventional power sources are impractical or unavailable. Their development not only contributes to the advancement of energy harvesting technologies but also aligns with global efforts to mitigate carbon emissions and transition towards a more sustainable energy landscape. Thus, research and innovation in nanogenerators play a pivotal role in shaping the future of renewable energy and powering the devices of tomorrow.

1.3 Problem Statement

The proliferation of portable electronic devices is hindered by persistent challenges such as the reliance on constant battery charging and the eventual degradation of battery performance over extended usage periods. To address these issues, there is a pressing need for the development of self-powered sensors capable of collecting external energy sources and efficiently converting them into electrical energy. Additionally, in light of growing environmental concerns and the imperative to minimize waste accumulation, the integration of green materials in self-powered sensor designs emerges as a preferable solution. However, the challenges associated with identifying suitable eco-friendly materials present a significant obstacle, requiring a delicate balance between performance requirements and environmental sustainability. The scarcity of appropriate green materials that can meet the

rigorous demands of sensor functionality while aligning with ecological principles further compounds this challenge. Thus, the pursuit of environmentally friendly alternatives adds another layer of complexity to the development of self-powered sensors, underscoring the need for comprehensive research and innovative solutions in material science and engineering.

1.4 Aim and Objectives

The goal of this project is to create an environmentally friendly self-sustaining sensor utilizing a nanogenerator energy harvesting system, incorporating eco-friendly materials for seamless integration into the Internet of Things. To fulfill this goal, specific objectives have been outlined:

1. To review on self-powered mechanisms and green materials
2. To fabricate a self-powered sensor using green materials
3. To integrate the self-powered sensor into the Internet of Things with Arduino

1.5 Scope and Limitation of the Study

The goal of the project is to create a self-powered sensor utilizing the triboelectric method specifically for Internet of Things application purposes. This project will be conducted to explore the behavior of triboelectric nanogenerators (TENG) in contact separation mode, with an emphasis on assessing the impact of chosen green materials. Other operational modes of TENG, such as freestanding and contact-sliding modes, will not be carried out due to concerns about material wear and complexity. Additionally, the scope of the study is limited to TENG's application as a sensor, neglecting its potential for energy harvesting or powering other small-scale electronics. The sensor design will be simplified by employing only two triboelectric materials on each side of the terminal, which may result in lower power output compared to previous research as the consistency of the sensor's performance may be affected when subjected to occasional tapping, rather than continuous tapping with a capacitor to store power as in previous studies. Furthermore, when compared to conventional materials, green triboelectric materials frequently show reduced mechanical robustness, stability, and output

performance. With repeated use, these environmentally acceptable substitutes—such as recycled materials and biodegradable polymers—may break down more quickly, which can cause a large decline in voltage output over a long period of cycles. Their innate mechanical flaws and vulnerability to external influences are blamed for this reduced performance, which has an impact on their long-term dependability and effectiveness in energy-collecting applications. As the energy harvesting function is not considered, the self-powered sensor will not supply power to the microcontroller, requiring an external power source.

1.6 Contribution of the Study

The study concentrates on developing a self-powered sensor that utilizes green materials, specifically emphasizing the triboelectric contact separation mode. Various materials are available in the market; however, paper, cloth, and PVC sheets were selected due to their ubiquity in everyday life, as well as their low cost and reusability. Arabic gum-graphite composite is employed as an electrode to replace copper. This substitution is favorable because the production of graphite electrodes, when enhanced with Arabic gum, generally results in a smaller environmental impact compared to copper production. Graphite can be synthesized or naturally mined with significantly less ecological harm than the extensive environmental degradation often associated with copper mining. Moreover, the biodegradable nature of both Arabic gum and graphite contributes to their environmental friendliness, thanks to their organic properties. Characterization processes allow for the examination and testing of the mechanical and electrical properties and performance of the newly developed self-powered sensor. The properties of the constructed sensor have been adapted for integration with IoT applications, demonstrating its potential utility in aiding the rehabilitation of elderly individuals.

1.7 Outline of the Report

There are five chapters within the report. The paragraph that follows will go through each chapter's contents.

The project backdrop, including the research's significance, problem description, goals and objectives, study scope and limitations, research

contribution, and study outline, will all be covered in Chapter 1. This chapter will give a quick overview of the field and explain why the project is being undertaken. The relevance of the project and some of its overall limits will be covered, along with green self-powered sensors.

Chapter 2 provides an overview of self-powered mechanisms that have been conducted to assess the benefits and drawbacks of each energy conversion method. Additionally, a review of various green materials employed by other researchers is included, along with the core principle underpinning TENG.

The project's approach and implementation plan, which are divided into four sections—fabrication, characterization, application planning, and electrode and dielectric material—are discussed in Chapter 3. This chapter discusses the apparatus and tools used.

In Chapter 4, the findings from characterization, mechanical and electrical properties, and IOT application are examined and addressed. The theory and properties of the green self-powered sensor are described.

Finally, Chapter 5 will wrap up the entire project with future work and suggestions for green self-powered sensors.

CHAPTER 2

LITERATURE REVIEW

2.1 Introduction

This section begins with an examination of existing literature on various self-powered mechanisms. It then delves into the theoretical principles behind different types of nanogenerators and explores the various operating modes of triboelectric nanogenerators (TENG). Factors influencing the performance of TENG are investigated and discussed. Additionally, the chapter provides a review of applications involving human-machine interaction.

2.2 Self-powered Mechanisms

Various energy harvesting techniques have been developed and applied extensively in human-machine interaction scenarios, serving as self-powered sensors for detecting diverse variables such as temperature, pressure, and strain. These mechanisms encompass a range of methods, including photovoltaic systems utilizing solar energy, electromagnetic generators, biofuel cells, radio-frequency technologies, thermoelectric generators, piezoelectric nanogenerators, and triboelectric nanogenerators. Potential energy sources for harvesting encompass electromagnetic energy from infrared, solar, or RF sources, mechanical energy acquired from vibrations or stress, thermal energy obtained from combustion engines, human energy from metabolic processes and activities, and sound energy (Sojan & Kulkarni, 2016). Utilizing various sensors, these energy sources can be harnessed and converted into usable electrical energy in the form of voltages and currents.

2.2.1 Photovoltaic

According to Hao et al. (2022), the researcher discussed the significance of tackling power supply challenges and mitigating environmental pollution by utilizing photovoltaic (PV) self-powered systems. These systems are categorized into four main types based on their specific application scenarios: personal wearables, transportation, household and building systems, and environmental monitoring equipment as shown in Figure 2.1. Despite this

classification, all PV self-powered applications share a common structure consisting of three essential components: a module of energy harvesting, a module of energy conversion, and a module of energy storage.

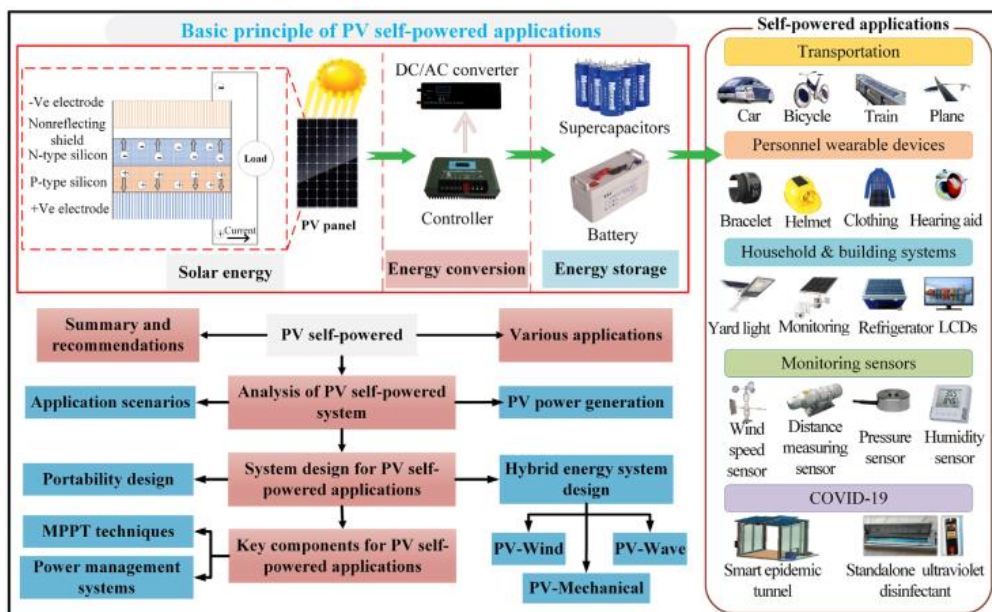


Figure 2.1: Principle of PV self-powered technologies. Reprinted with permission from copyright 2022 Elsevier.

PV cells, also referred to as solar cells, operate by converting sunlight directly into electricity through the photovoltaic effect. When sunlight interacts with the PV cells, the semiconductor material within absorbs photons, resulting in the generation of an electric current as electrons are dislodged from their atoms. This electric current can then be utilized as electrical energy to power various devices and applications.

However, PV self-powered systems encounter certain limitations. For instance, their design necessitates maintenance to maintain efficiency, including routine cleaning and periodic repairs. Additionally, challenges such as the inability to maximize power output under partial shading conditions pose constraints on their efficiency and reliability.

2.2.2 Electromagnetic Generator

The primary element of Electromagnetic Generators (EMGs) consists of coils and magnets positioned within a magnetic field. EMGs function according to

the inductive electromagnetic principle, which states that a conductor moving through a magnetic field will produce an electromotive force, thereby generating electricity. In the context of wind energy harvesting, EMGs utilize the mechanical energy derived from the motion of magnets and coils induced by the wind to produce electrical energy. However, EMGs are often characterized by their rigidity and bulkiness, primarily due to material limitations. Additionally, the wear and tear of moving components pose challenges in their maintenance and longevity.

The Water-Proof Triboelectric-Electromagnetic Hybrid Generator (WPHG) is engineered for energy harvesting in challenging environments as shown in Figure 2.2. Integrating the concepts of triboelectrification and electrostatic induction, this generator produces electricity efficiently (Guo et al., 2016). Encased in a fully sealed enclosure, it is safeguarded against water and other adverse conditions, rendering it suitable for diverse practical applications.

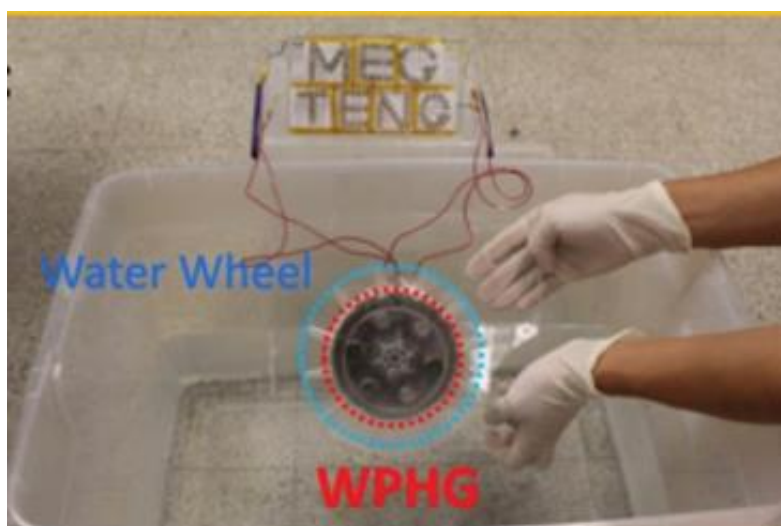


Figure 2.2: Practical of the water-proof hybrid generator. Reprinted with permission from copyright 2015 Advanced Energy Materials.

2.2.3 Biofuel Cells

Biofuels are abundant within the human body, residing in fluids or organs in various forms such as lactate, glucose (recognized as the primary fuel for human cells), ascorbic acid (vitamin C), urea as a waste product, ethanol, disaccharide trehalose composed of two glucose molecules, fructose, and

others. Utilizing enzyme-accelerated electrochemical reactions, biofuel-based harvesters have the capability to convert the chemical energy directly from these energy-producing substances within the body into electrical energy (Farzin et al., 2024).

In a Biofuel Cell, the biofuel (like glucose or other biomolecules) undergoes oxidation at the anode with the assistance of biocatalysts, resulting in the release of electrons. These electrons subsequently traverse an external circuit towards the cathode. At the cathode, an oxidant (typically oxygen) experiences reduction, completing a closed circuit. This mechanism generates an electric current determined by the potential disparity between the reactions transpiring at the anode and cathode, ultimately yielding electrical power as shown in Figure 2.3. Nonetheless, the biochemical reactions that produce electricity in biofuel cells generally proceed at slower rates compared to the chemical reactions in conventional batteries.

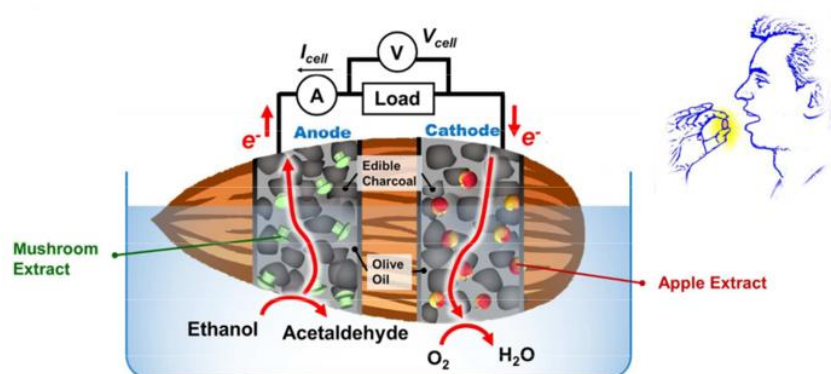


Figure 2.3: Anode and cathode pastes that are completely edible are contained inside a hollow almond to form an implantable ethanol biofuel cell. Reprinted with permission from copyright 2024 ASC Biomaterials Science & Engineering.

2.2.4 Radio-frequency

Radio-frequency (RF) energy harvesters, comprising components like antennas, optional matching networks, RF-DC converters with ultra-low-power, and output loads, utilize radio waves to produce electricity as shown in Figure 2.4. These devices transform incoming RF energy into DC energy, facilitating battery-free operation for wireless sensor nodes in IoT applications

(Rahmani et al., 2023). However, radio frequency signals are prone to interference and noise, potentially affecting the efficiency of energy harvesting systems.

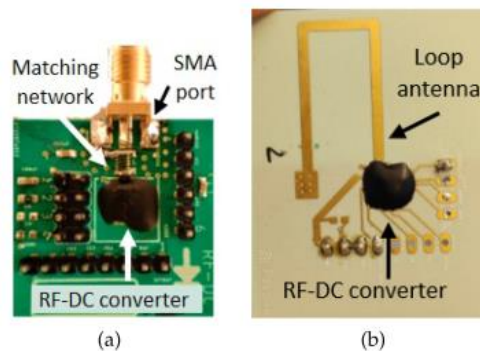


Figure 2.4: (a) Matching network with 50Ω antenna and (b) matched single-ended loop antenna. Reprinted with permission from copyright 2023 IEEE.

2.2.5 Thermoelectric Generator

According to Liu et al. (2023), the researcher explores the advancement of flexible, robust, and eco-friendly thermoelectric composite fabrics designed for energy harvesting to become self-powered sensors in wearable textiles. The researcher employed an innovative fabrication approach, combining carbon nanotube electrospray with polylactic acid (PLA) fabric electrospinning to produce TE composite fabrics as illustrated in Figure 2.5. These fabrics exhibited significant Seebeck coefficient and power density, facilitating effective electricity generation from body heat and enabling breath and temperature sensing. The study underscores the durability of these thermoelectric (TE) fabrics and their potential utilization in wearable electronic devices.

Thermoelectric materials operate based on the Seebeck effect, wherein a temperature difference within the material prompts the motion of charge carriers, resulting in the production of an electric current. By heating one side of the material while cooling the other, a voltage difference is established, facilitating the transformation of heat energy into electrical energy. Nevertheless, the study did not address the selection of mechanical motions suitable for conversion into electrical energy.

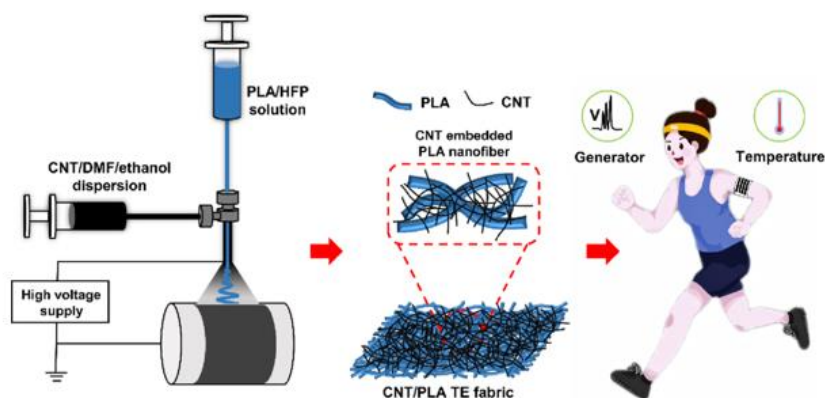


Figure 2.5: Design of CNT/PLA TE composite fabric and its function in wearable TE generators and temperature sensing. Reprinted with permission from copyright 2023 Composites Science and Technology.

2.2.6 Piezoelectric Nanogenerator

Unlike the previously discussed energy harvesting devices, the piezoelectric nanogenerator (PENG) transforms mechanical energy, such as pressure or vibrations, into electrical energy. Within a composite nanogenerator containing piezoelectric elements like ZnO nanowires, the mechanical energy produced by external stimuli, such as palm impacts or foot stamps as outlined in Figure 2.6, undergoes conversion into electrical energy (Saravanakumar et al., 2015).

When the ZnO nanowires within the composite experience external mechanical deformation, such as palm impacts or foot stamps, they incur compressive strain through the polydimethylsiloxane (PDMS) polymer. This strain leads to the division of stationary charge centers in ions along the surface of the ZnO nanowires, thereby establishing a piezoelectric potential gradient. Consequently, a piezo potential emerges across the electrode surface, propelling electrons within the external circuit and producing an output voltage and current. Upon removal of the external force, the piezo potential dissipates, causing electrons to travel across the outside circuit in the reverse direction to preserve charge neutrality, thereby generating a reverse signal. However, piezoelectric materials are not flexible and are prone to cracking under stress.



Figure 2.6: Digital image of the foot stamp at different stages. Reprinted with permission from copyright 2015 Elsevier.

2.3 Triboelectric Nanogenerators

Triboelectricity is a familiar electrostatic phenomenon that we encounter regularly in our daily lives. It occurs when two different materials with distinct electrostatic properties come into physical contact. Upon contact, one material turns negatively charged and positively charged for another. When these materials are split, a net potential difference is created between them. This separation leads to opposite charges on the surfaces of the materials due to electrostatic induction. As a result, a potential difference is established when the materials are split by an external mechanical force. This process also causes an electron flow between the electrodes, generating an alternating current (AC) output (Lai et al., 2022).

2.3.1 Four Working Modes for Triboelectric Nanogenerators

There are four primary modes of triboelectric nanogenerators: vertical contact separation mode, single electrode mode, sliding mode, and free-standing mode. In the vertical contact separation mode Figure 2.7 (a), which is a simple configuration of a TENG, two dielectric films with electrodes behind them come into frictional contact. Due to their different electron affinities, they develop oppositely charged surfaces. Applying an external force separates these surfaces, creating a potential difference between the electrodes. This difference generates a current across a load, producing an alternating current (AC) output when the films repeatedly contact and separate.

The sliding mode Figure 2.7 (b) involves two layers with opposite triboelectric polarities initially in full contact, resulting in equal and opposite charge densities. When an external force is applied, in relation to the bottom

layer, the top layer glides, reducing its contact area and separating the charges. This separation produces a potential difference that drives electron travel between the electrodes at the bottom and top until the layers are fully separated. Reverse motion can cause reverse electron flow until electrostatic equilibrium is reached.

The single electrode mode Figure 2.7 (c) features a movable contact layer that can move freely without a connection. This mode is composed of a moveable contrasting layer and a ground electrode. A potential difference is created when the moveable layer periodically comes into touch with itself and separates, leading to electron flow between the electrode and the ground.

The free-standing mode Figure 2.7 (d) operates in a non-contact manner with two symmetric electrodes beneath a dielectric layer separated by a small gap. Initially charged during the triboelectric process, the movable layer's movement toward and moving away from the electrodes results in an uneven distribution of charges. This asymmetry drives electron flow between the electrodes, producing an AC output.

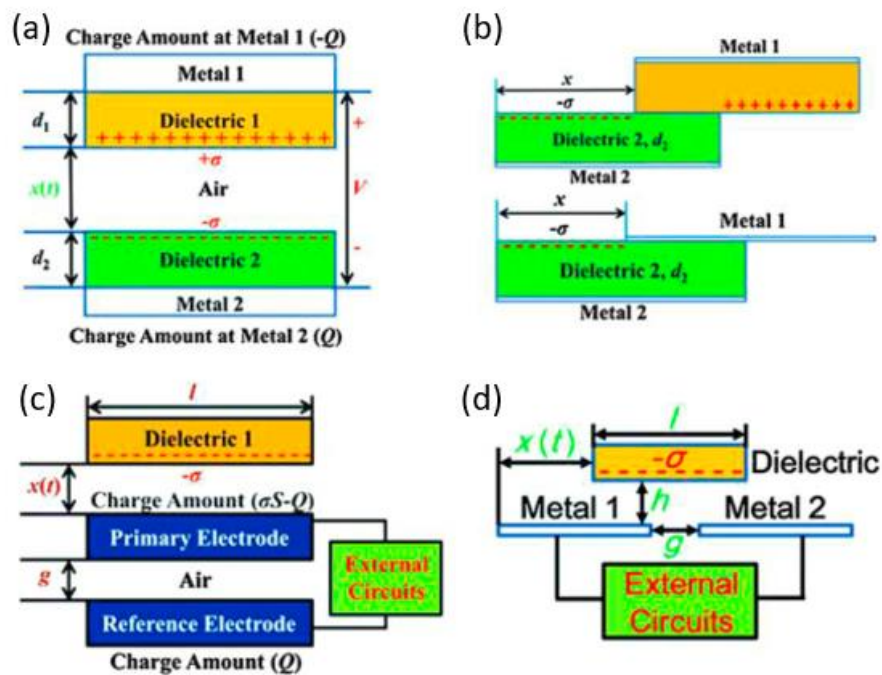


Figure 2.7: (a) Vertical contact separation mode, (b) sliding mode, (c) single electrode mode, and (d) free-standing mode. Reprinted with permission from copyright 2022 Joule.

2.3.2 Triboelectric Series

It is important to understand that not all materials can hold or accept charge in the same way; their capacity to hold charge varies. Additionally, a material's ability to attract or release electrons depends on its inherent nature. To provide a reference point for this behavior, an empirical triboelectric series is presented in Figure 2.8. Materials listed on the left column of this series possess a great potential to pick up a net positive charge once interacting with the elements below, indicating that these materials are good electron donors. Conversely, materials on the right column tend to acquire a net negative charge and are thus good electron acceptors. Materials with a higher tendency to donate or accept electrons also have a greater capacity to store charges compared to those lower on the list. This results in a higher surface charge density on the material after friction, meaning it can either donate or accept more electrons. Therefore, the triboelectric series serves as a valuable tool for predicting both the polarity and magnitude of charge separation (Lai et al., 2022). Table 2.1 displays environmentally friendly materials that are both biodegradable and recyclable, sourced from the Empirical Triboelectric Series.

POSITIVE CHARGE		NEUTRAL	NEGATIVE CHARGE	
	Dry Human skin	Cotton		Wood
	Leather	Steel		Amber
	Rabbit Fur			Hard rubber
	Glass			Nickel, Copper
	Quartz			Brass, Silver
	Human hair			Gold, Platinum
	Nylon			Polyester
	Wool			Saran Wrap
	Lead			Polyurethane
	Fur			Polyethylene
	Lead			Polypropylene
	Silk			Vinyl (PVC)
	Aluminum			Silicon
	Paper			Teflon

Figure 2.8: Empirical Triboelectric Series. Reprinted with permission from copyright 2022 Joule.

Table 2.1: Green Materials from Empirical Triboelectric Series.

Triboelectric Charge	Biodegradable	Recyclable
Positive Charge	Dry human skin Leather Rabbit fur Wool Fur Silk Paper Cotton	Glass Nylon Aluminium
Negative Charge	Wood Amber	Steel Nickel, copper Brass, silver Gold, Platinum Polyester Polyethylene Polypropylene Vinyl (PVC) Silicon Teflon

2.3.3 Green Dielectric Material

The researchers have developed biodegradable triboelectric nanogenerators (BD-TENGs) using gelatin film and electrospun polylactic acid (PLA) nanofiber membranes as shown in Figure 2.9. Through optimizing the properties of these eco-friendly and biocompatible materials, the BD-TENGs demonstrate impressive performance, including an output voltage of 500 V, a short-circuit output current density of 10.6 mA/m², and an optimal density of power greater than 5 W/m² with a dimension size of 4 × 4 cm². The incorporation of gelatin and PLA in the BD-TENGs highlights their potential for sustainable energy harvesting applications.

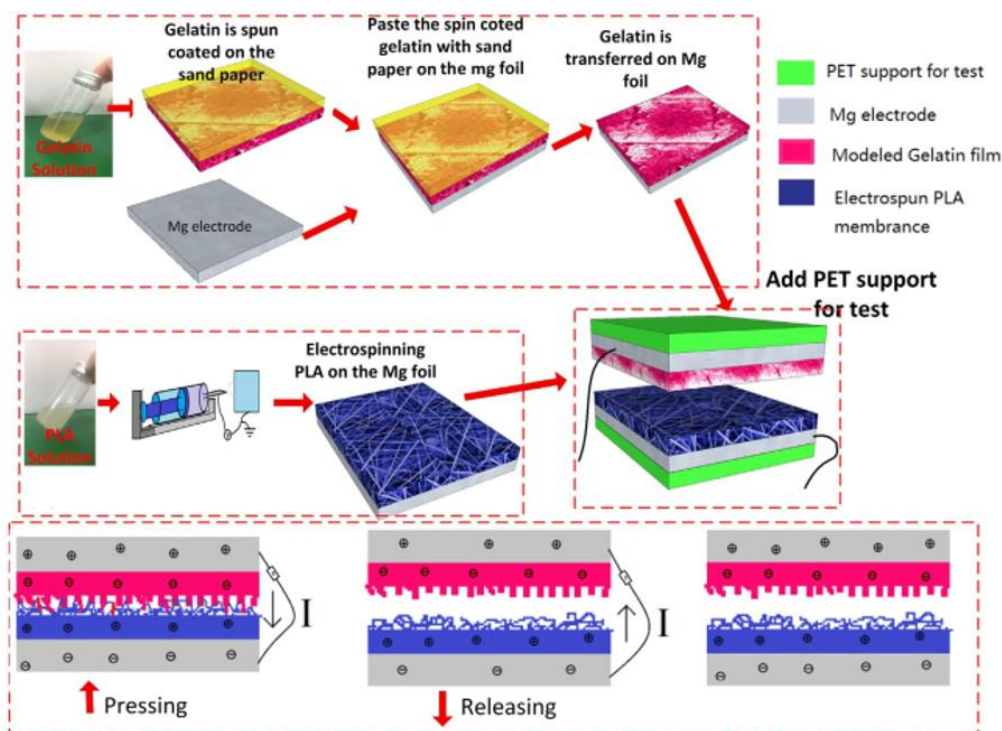


Figure 2.9: Production method of PLA and gelatin plates. Reprinted with permission from copyright 2018 Elsevier.

According to Pan et al. (2018), the biodegradability of materials used in energy harvesting devices is crucial, highlighting the importance of materials that can break down naturally without causing environmental harm. The selection of gelatin and PLA as tribo-materials for BD-TENGs offers several advantages due to their biocompatibility, biodegradability, and appropriate electron affinities for efficient energy conversion. Adding magnesium (Mg) as the electrode material further boosts the eco-friendliness of the BD-TENGs. Mg is not only biocompatible but also highly conductive and can dissolve without posing any environmental or health risks. The complete dissolution time for the PLA nanofiber is around 40 to 45 days as demonstrated in Figure 2.10. Despite its usefulness, gelatin is extremely sensitive to moisture, which can have an impact on how stable and effective it is in humid conditions. Over time, this sensitivity may lead to deterioration, potentially reducing the lifespan of devices.

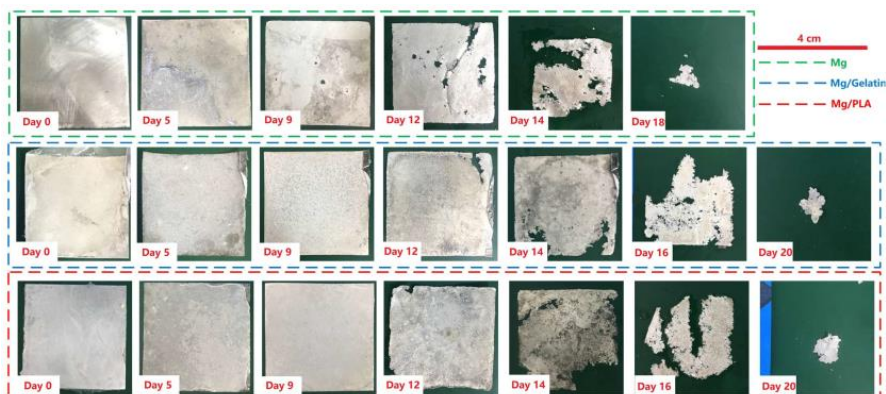


Figure 2.10: Photos of the disintegrating PLA/Mg sheets, Mg foil, and gelatine/Mg in natural water. Reprinted with permission from copyright 2018 Elsevier.

A researcher has developed a new Triboelectric Nanogenerator (TENG) design that employs polytetrafluoroethylene (PTFE) film and a bamboo leaf layer for the triboelectric layers, aiming at biomechanical energy harvesting and self-powered touch-sensing (Xu et al., 2024). The bamboo leaves provide benefits like cost-effectiveness, availability, non-toxicity, and environmental friendliness. Experimental optimization of the triboelectric performance of bamboo leaves led to a TENG device with remarkable power output and voltage properties. However, bamboo leaves generally have a short lifespan because they decompose quickly.

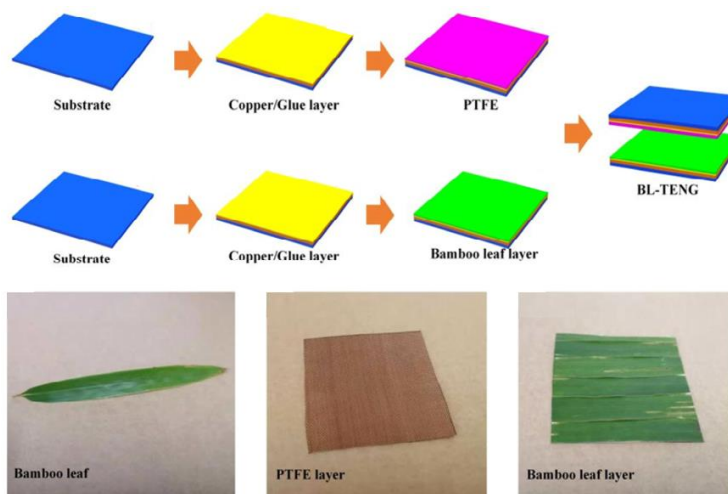


Figure 2.11: Fabrication process of bamboo leaf and polytetrafluoroethylene (PTFE) film. Reprinted with permission from copyright 2024 MDPI.

Using recycled plastic and paper as green dielectric materials and graphite electrodes made from electronic waste (dry cells), a researcher has created an affordable and ecologically friendly triboelectric nanogenerator (TENG) (Bukhari et al., 2022). The study focused on the serious ecological concerns associated with the accumulation of non-recycled plastics, particularly bottles, and electronic waste, which contribute to environmental problems. This creative strategy emphasizes the critical role that recycling and reuse play in creating a more sustainable future by promoting renewable energy generation in addition to trash management. Since paper material decomposes more slowly than bamboo leaves, it is preferred.

2.3.4 Green Electrode Material

The researchers employ flexible conductive dough in place of traditional wires, offering straightforward circuit-building activities. A basic circuit can be assembled in Squishy Circuits using a battery pack, two blobs of conductive dough, and an LED. In this setup, electricity travels from the battery's positive terminal through the first dough blob, passes through the LED, moves through the second dough blob, and returns to the battery's negative terminal. Current flows through materials known as conductors. While not all materials can conduct electricity, substances like salt and water are excellent conductors. The salt content in the playdough makes it capable of conducting electricity as presented in Figure 2.12. However, the dough needs to be moist so that ions can move freely to conduct electricity, as it is not effective in its dry state (Peppler et al., 2019).



Figure 2.12: Simple circuit conductive dough with LED. Reprinted with permission from copyright 2018 Springer Nature.

Other researchers have investigated pencil drawings on paper as a straightforward and cost-efficient approach to crafting electronic devices. They utilize the conductivity of graphite in pencil lines to create various applications, including sensors, energy storage systems, and active components like field-effect transistors. Additionally, they stress the potential of these pencil-on-paper electronics in producing lightweight, flexible, and disposable electronic devices for a range of uses. Moreover, the researchers point out the benefits of pencil-on-paper electronics, such as easy fabrication, affordability, and eco-friendliness. By using pencil sketches as conductive paths and active components, they have shown that it's possible to make paper-based electronic devices with desirable features. The absence of solvents in pencil-on-paper electronics streamlines the manufacturing process, making it suitable for environmentally friendly electrode materials (Kurra & Kulkarni, 2013). Nevertheless, the graphite that the pencil applied may corrode or deteriorate with time, reducing the conductivity of the carbon lines on the paper. Handling, friction, and other environmental conditions can hasten this degradation, which will eventually make the pencil-on-paper electronic circuits less functional.

Some researchers are exploring the reuse of waste coffee grounds (WCG) as electrode materials as shown in Figure 2.13, showcasing recent progress and potential future developments in this area. As electrodes, they exhibit promising electrochemical properties and have been utilized in capacitors/supercapacitors, batteries, and electrochemical sensors due to their affordability, high electrical conductivity, polarization, and chemical stability (Pagett et al., 2023).

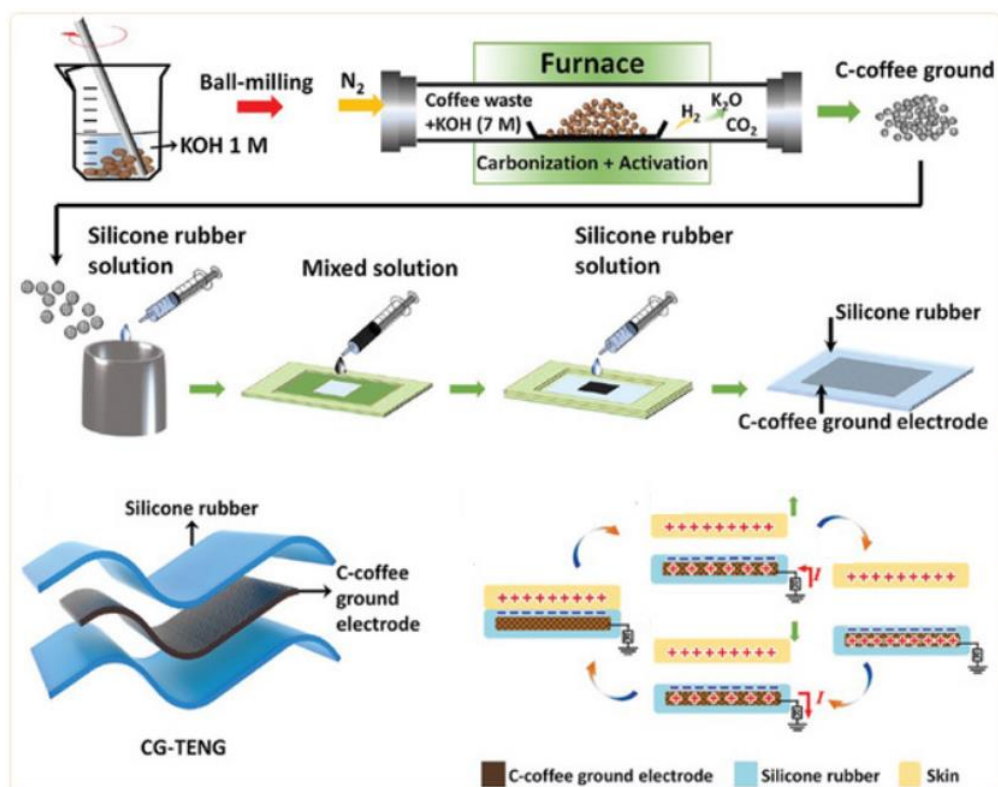


Figure 2.13: Fabrication for WCG-derived TENG. Reprinted with permission from copyright 2022 Global Challenges.

Based on Li et al. 2023 copper adhesive tapes serve as electrodes in constructing the droplet-based triboelectric nanogenerator (DTNG). They are affixed to both the upper and lower surfaces of the polydimethylsiloxane (PDMS)-PTFE films to create the device's electrodes. These copper electrodes are essential for producing electrical output through the interaction with water droplets, enabling the sensor's self-powered operation. By using cost-effective and environmentally friendly materials like PTFE film and copper foil, the device offers significant cost benefits when scaled up for large-scale deployment.

A technique for making graphite conductive paint and using it to create resistive-capacitive (RC) circuits on paper has been developed by other researchers. This method uses graphite powder, gum arabic as a binder, and water as a carrier to create conductive paint in an easy and inexpensive manner. To make a uniform paste, the preparation procedure entails heating water, dissolving gum arabic, and combining graphite. Because of its well-known non-toxicity and simplicity of application, the paint is appropriate for

educational settings, especially those including laboratories. The paint's ohmic qualities are highlighted in the article; it can be used effectively in circuit elements because of its typical resistance of about 30Ω per unit thickness (Preparation of Graphite Conductive Paint and Its Application to the Construction of RC Circuits on Paper, 2016). Given that Arabic gum-graphite composite is regarded as a green substance, it is the material of choice. Because graphite contains carbon, which is easily manufactured from a variety of materials by carbonization, graphite has the ability to conduct electricity. As long as enough carbon is retained, the Arabic gum-graphite composite can be reused several times by putting it in a liquid state with water, letting it dry, and allowing it to reconfigure without losing electrical conductivity. A major step forward in the creation of completely environmentally friendly electrical components is the development of electrodes free of metal.

2.4 Summary

This section has examined the operational theory and compared several self-powered devices. The comparison demonstrates that triboelectric energy harvesting offers a unique combination of adaptability, affordability, scalability, environmental friendliness, reliability, and noiseless operation. It can scale from small devices to large structures, utilize cost-effective materials, and adapt to various scenarios. Triboelectric energy harvesting is a dependable green technology, that provides a quiet and clean energy source that can power a diverse range of applications. Among self-powering technologies, it stands out as an exceptional option.

CHAPTER 3

METHODOLOGY AND WORK PLAN

3.1 Introduction

The materials and techniques used in the project are thoroughly examined in this chapter. A detailed discussion of the apparatus used for prototype testing is also included. To choose the right material, assess the behavior of the sensor, and determine which kind of sensor performs best, a few prototypes of the Triboelectric Nanogenerator (TENG) will be built. The properties of the TENG and its potential applications will be investigated in more detail through this prototype. Two applications for human-machine interaction will be designed to demonstrate the prototype's possible usage once testing results provide insights into the prototype's behavior.

3.2 Fabrication of Self-powered Sensor

The prototype was completed using the most straightforward method, which involved pressing and cutting the dielectric and electrode material to the correct dimensions. This approach also proved to be the most cost-effective means of fabricating the prototype, making it both practical and economical for the development of the triboelectric self-power sensor.

3.2.1 Dielectric Material

The triboelectric contact-separation mode in this prototype utilizes three dielectric materials which are reused polyvinyl chloride (PVC) sheets from bookbinding covers, recycled A4 paper, and biodegradable cotton cloth. Among these, the positive dielectric materials cloth and paper are selected based on their commonality in daily life, allowing for a comparative analysis of which material generates a higher potential difference when paired with copper electrodes. The PVC serves as the constant negative dielectric material in this setup, enabling comparisons between PVC and both cloth and paper. The material that produces the highest output voltage when paired with PVC will be chosen for attachment to the electrode, forming a green self-powered

system. The customized material arrangement based on the triboelectric series is shown in Figure 3.1.

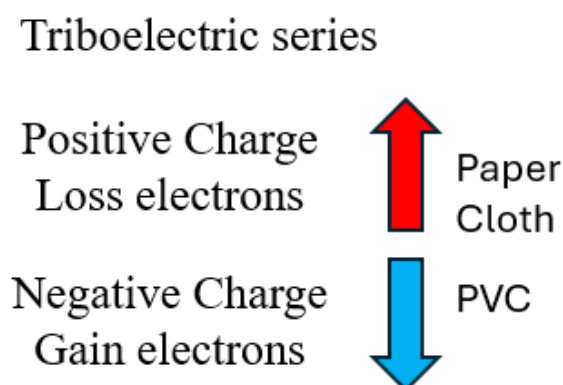


Figure 3.1: The triboelectric series includes paper, cotton, and PVC.

3.2.2 Preparation of Arabic Gum-Graphite Composite Electrode

Arabic gum serves as a vital binder in the production of graphite electrodes, ensuring that the graphite particles adhere effectively. Graphite, as the primary conductive material, provides the necessary electrical conductivity essential for the electrode's operation. Water functions as a critical solvent in this mixture, aiding in the complete dissolution of the Arabic gum powder and enabling it to uniformly coat the graphite particles. After mixing, the solution is stirred with a spoon for 5 minutes to ensure even distribution. The weight ratios of Arabic gum to graphite—5:10, 10:10, 15:10, and 20:10—require water volumes of 8 ml, 12 ml, 16 ml, and 20 ml, respectively. The prepared mixture is then applied to an A4-sized paper, with a marker outlining a 50mm x 50mm area, and a jumper wire is attached. A PVC sheet is placed on top of this coated area and pressed to achieve a thickness of 2mm. The assembly is left to dry in a ventilated room for 2 days, after which the electrode shape is cut out from the 50mm x 50mm area, completing the electrode preparation process.

3.2.2.1 Mechanical and Electrical Properties of Electrode

The Arabic gum-graphite composite electrodes, prepared with different weight ratios, were subjected to mechanical testing using the Instron 5582 testing machine, operated with Instron Bluehill Software, as shown in Figure 3.2.

Each electrode sample was placed between two supports, with a span distance of 3 cm. A central load of 10N was applied to the sample, and the bending speed was maintained at 2mm/min. During the test, the deflection of the electrode was carefully recorded.

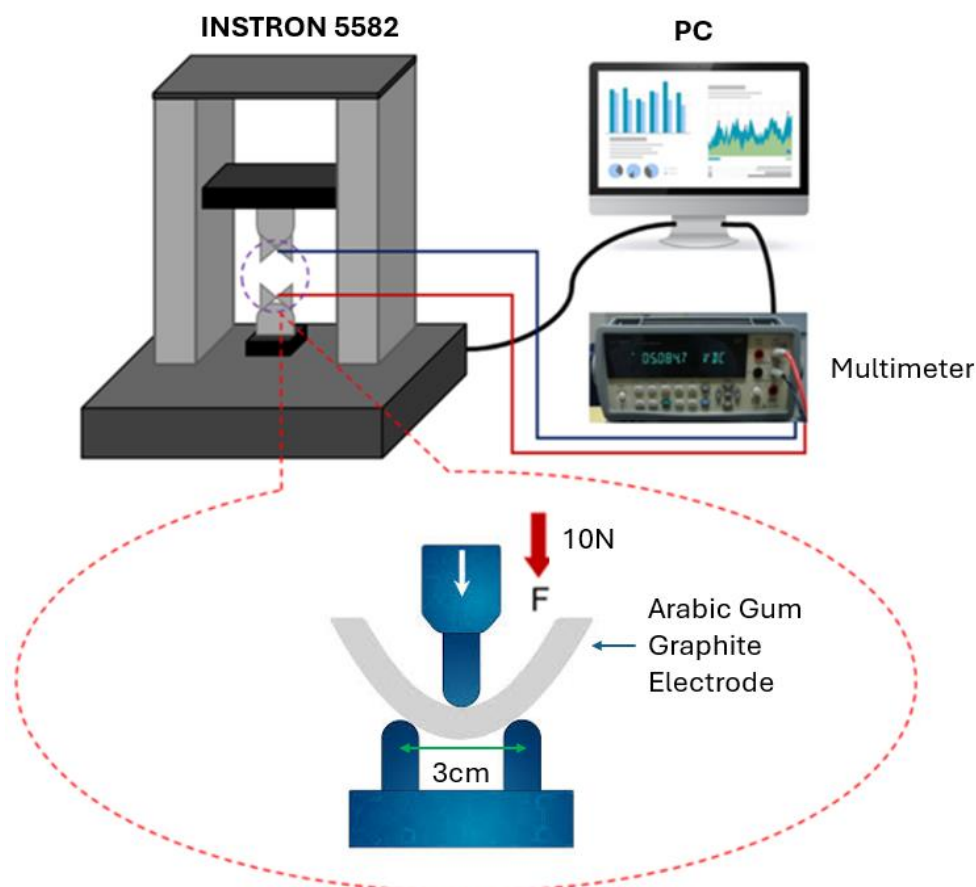


Figure 3.2: Electrode bending test.

The recorded deflection data were then applied to the deflection equation used in a three-point bending test to calculate Young's modulus of the electrode samples, as referenced in Equations 3.1 and 3.2 (Abbott, 2009). This calculation provides a measure of the stiffness and elasticity of the material. Finally, the Young's modulus values obtained for the Arabic gum-graphite composite electrodes were compared with the Young's modulus of a standard copper sheet, allowing for an assessment of the mechanical properties and potential performance of the electrodes relative to the well-known copper material.

$$I = \frac{bh^3}{12} \quad (3.1)$$

$$\delta = \frac{FL^3}{48EI} \quad (3.2)$$

where

I = moment of inertia, m^3

b = width, m

h = thickness, m

δ = deflection, m

F = force, N

L = length, m

E = young's modulus, Pa

The resistance of each Arabic gum-graphite composite electrode was measured using a multimeter, employing a two-probe method with a distance of 1.5 cm between the probes. The measured resistance values were then applied to the conductivity equation with a cross-sectional area of 1 cm^2 , as shown in Equation 3.3, to determine the electrical conductivity of the electrodes. The electrode with the lowest stiffness and highest electrical conductivity will be chosen, contributing to the formation of an environmentally friendly self-powered system.

$$\sigma = \frac{1}{R} \times \frac{l}{A} \quad (3.3)$$

where

σ = electrical conductivity

R = resistance, ohm

l = distance between the probes, cm

A = cross-sectional area, cm^2

The Scanning Electron Microscope (SEM) analysis will be conducted using the S-3400N machine. The surfaces of both the copper sheet and the Arabic gum-graphite composite with the highest electrical conductivity will be

prepared and analyzed to assess their surface roughness characteristics. Samples measuring 1 cm x 1 cm will be precisely cut and mounted on conductive stubs using carbon tape. This ensures optimal conductivity and minimizes charging effects during imaging, as displayed in Figure 3.3. The SEM will be operated under high vacuum conditions, with magnification and brightness settings carefully adjusted to capture detailed surface features. The resulting images will provide valuable insights into the surface roughness, enabling a comparative analysis between the copper sheet and the Arabic gum-graphite composite to determine which is rougher. A rougher surface increases the contact area between the dielectric and the electrode, which can lead to higher voltage production.

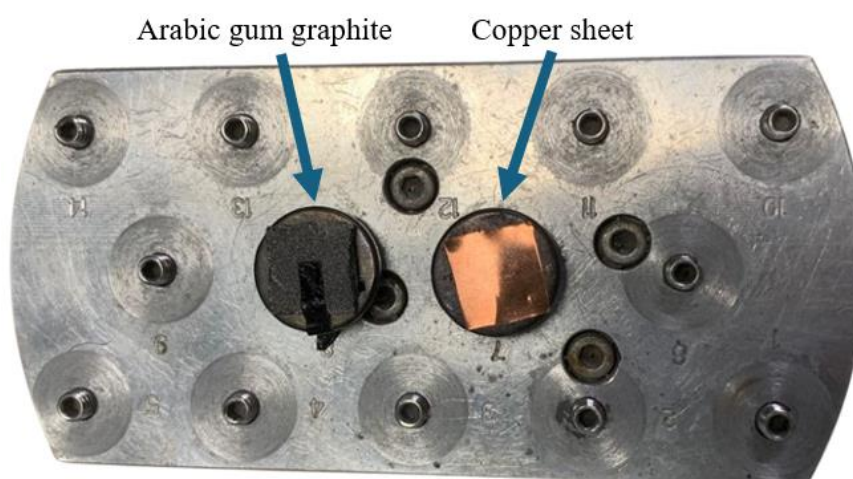


Figure 3.3: Arabic gum-graphite composite and copper sheet samples on SEM sample holder.

3.3 Fabrication Process of Green Self-powered Sensor

Copper is commonly used in electronic devices due to its high electrical conductivity, which makes it an ideal material for electrodes. In this fabrication process, a copper sheet with a thickness of 0.06 mm is selected and cut into dimensions of 50 mm x 50 mm. This copper sheet serves as the base for the electrode. A positive dielectric material, such as paper or cloth, is attached to one side of the copper sheet, while a negative dielectric material, like a PVC sheet, is attached to another copper sheet of the same thickness and dimensions. Both copper sheets are fitted with two jumper wires, which are soldered in place for electrical connections. These copper sheets, with their

respective dielectric materials, are then attached to the top and bottom of a flat arch structure cover.

For another sensor with different electrode materials, a mixture of Arabic gum and graphite powder is prepared by stirring them together with a spoon. This conductive mixture, along with an additional jumper wire, is placed between the paper or cloth and PVC layers. Before curing, the mixture is pressed until it reaches a thickness of 2mm. Once the material has set, it is cut to a 50mm x 50mm dimension. This layer is then securely attached to the flat arch structure cover. With these steps completed, the fabrication of this version of the self-powered triboelectric sensor in contact-separation mode is completed, according to Figure 3.4.

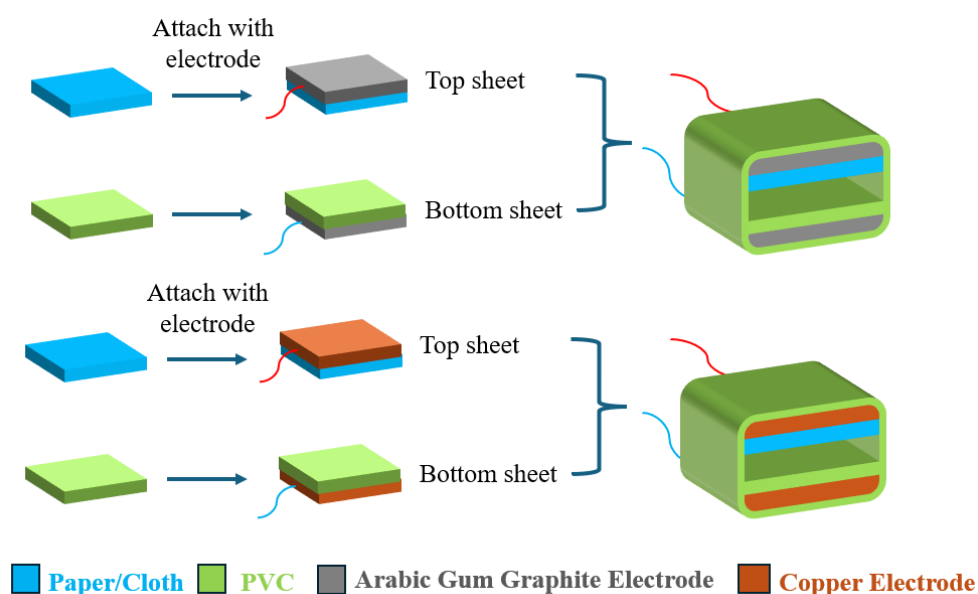


Figure 3.4: Fabrication process.

3.4 Characterization of the Self-powered Sensor

A digital multimeter will be used to measure the output voltage in order to characterize the self-powered sensor. The electrode can be connected to the digital multimeter to obtain data from the sensor. The main objective of utilizing this apparatus is to directly transmit data from the sensor to a computer for additional analysis and application development.



Figure 3.5: Digital multimeter.

Initially, under a copper electrode, comparisons between cloth and paper will be conducted for sensor characterization. Using PVC as a consistently triboelectric negative material will aid in determining which material exhibits greater triboelectric positivity by comparing the potential difference produced under the same force of 10 N and a gap distance of 3 cm. Subsequently, the material that is more triboelectrically positive is chosen to be attached to the Arabic gum-graphite composite electrode, which exhibits the highest and lowest electrical conductivity among the varying weight ratios. This will replace the copper electrode and will be tested under the same force of 10 N and a gap distance of 3 cm to evaluate the potential differences generated. The most effective green material, which generates the highest potential difference, will be selected for further characterization tests. Following this, different loads of 10 N, 20 N, and 30 N will be applied at a fixed height of 3 cm to test the self-powered sensor and simulate various force levels acting on it. It will be possible to obtain and graphically portray a comprehensive understanding of the sensor's response to different forces by recording the average output voltage for each level. Additionally, the sensor will be tested at varying gap lengths of 1 cm, 2 cm, and 3 cm, while maintaining a constant force of 10 N, and the average output voltage will be recorded at each distance. Finally, a durability test consisting of a thousand cycles will evaluate the voltage output stability and longevity of the sensor under a force of 10 N and a gap length of 3 cm. An Instron Micro Tester, which regulates the force and gap distance in contact-separation mode, will be used to detect voltage, as demonstrated in Figure 3.6. The input frequency will be set to 0.5 Hz to avoid overheating the servo motor.

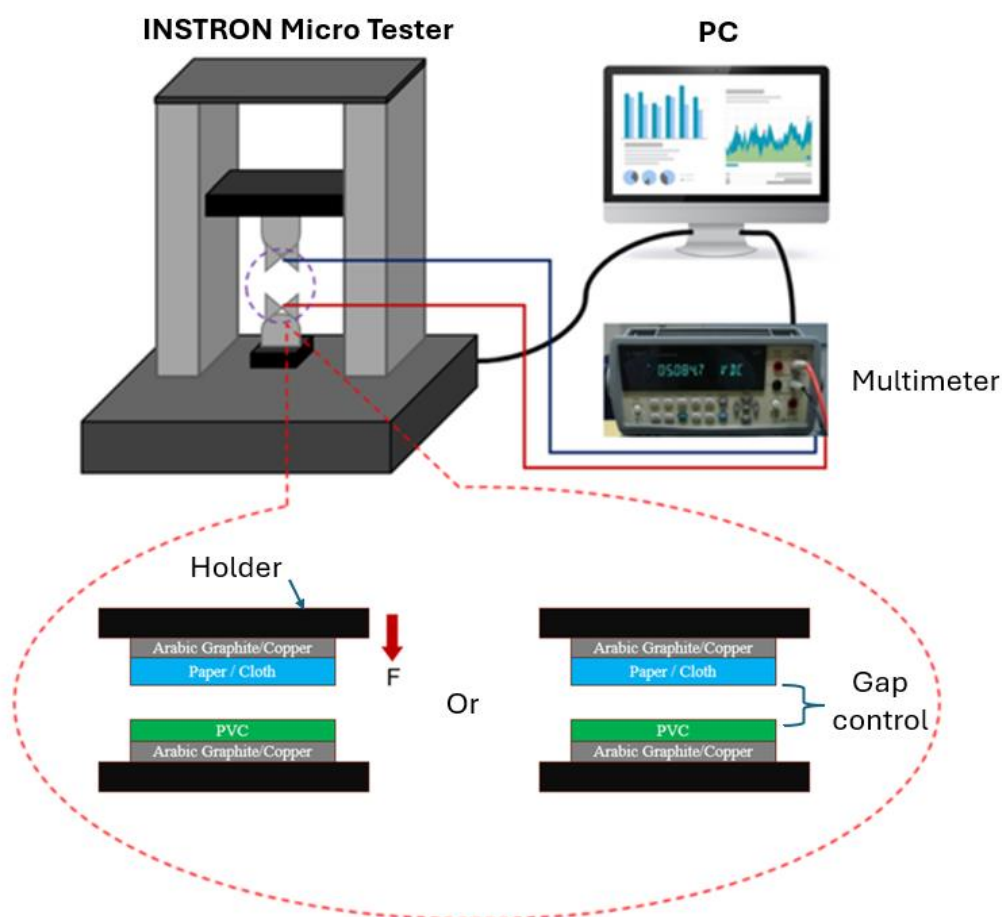


Figure 3.6: Machine tapping test.

3.5 Internet of Things

The integration of a self-powered sensor into the Internet of Things (IoT) involves connecting the sensor to a network, enabling it to wirelessly transmit data to other devices or cloud-based platforms. In this context, a Ping Pong game has been implemented on the ESP32 microcontroller and an Organic Light Emitting Diode (OLED) display, specifically designed for elderly individuals. The game requires the user to tap the sensor with their hand, which controls the movement of the Ping Pong paddle, allowing it to move left or right. Conceptually, the scoring marks achieved by the patient are recorded and transmitted via Blynk (IoT) over WiFi to the doctor's phone or laptop. This real-time data transmission enables the doctor to monitor whether the patient has met the targeted score without needing to physically visit the patient to instruct them on performing small exercises. The primary objective of this game is to assist in the rehabilitation of elderly individuals by improving their response times through engaging and interactive gameplay.

For the electrical circuit illustrated in Figure 3.7, each sensor electrode, with a positive dielectric material attached, is connected to analog input pin 35 to control the paddle's upward movement, and to another analog input pin 34 to control the paddle's downward movement. The electrode with the negative dielectric material is connected to the ground. Additionally, the SCL and SDA lines from the 128 x 64 OLED display are connected to the corresponding pins on the ESP32.

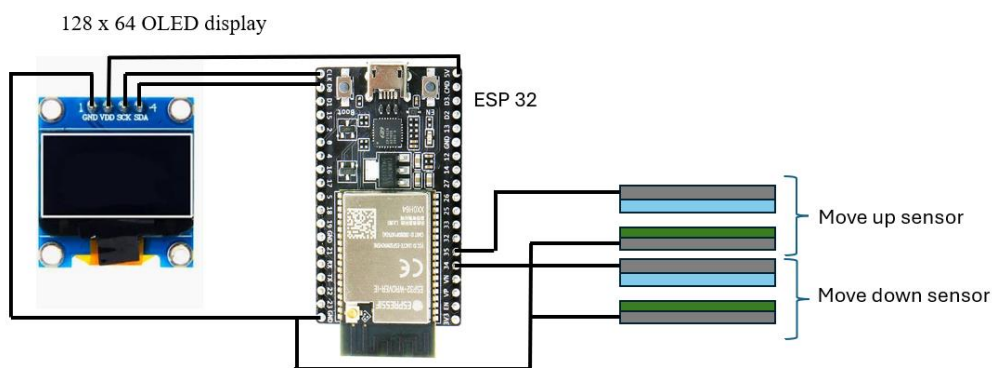


Figure 3.7: Circuit diagram for ping pong game.

3.6 Gantt Chart

Table 3.1 and Table 3.2 indicate the project operations completed for both FYP1 and FYP2.

Table 3.1: FYP1 Gantt Chart

Gantt Chart Part-1															
No.	Project Activities	W1	W2	W3	W4	W5	W6	W7	W8	W9	W10	W11	W12	W13	W14
M1	Problem formulation & Project planning	█	█												
M2	Literature review		█	█	█	█	█	█	█						
M3	Preliminary testing/investigation with data gathering							█	█	█	█	█	█		
M4	Report writing & presentation												█	█	█

Table 3.2: FYP2 Gantt Chart

Gantt Chart Part-2															
No.	Project Activities	W1	W2	W3	W4	W5	W6	W7	W8	W9	W10	W11	W12	W13	W14
M1	Purchase and prepare required materials	■	■	■											
M2	Fabricate the prototype sensor		■	■	■	■	■								
M3	Testing and analysis the sensor				■	■	■	■	■	■	■				
M4	Finalising report writing and presentation							■	■	■	■	■	■	■	■

3.7 Summary

In summary, a self-powered sensor utilizing green materials has been fabricated. The contact-separation mode in the triboelectric nanogenerator was tested using paper and cloth as the contact materials, and copper and Arabic gum-graphite composite as the electrode materials. Following these tests, the optimal dielectric material and electrode were selected for the final prototype. The prototype was assembled using simple pressing and cutting techniques. The sensor was then characterized using a digital multimeter. Finally, an IoT-based Ping Pong game was designed using the sensor integrated with an ESP32 microcontroller.

CHAPTER 4

RESULTS AND DISCUSSION

4.1 Introduction

This chapter begins by presenting practical tests on the mechanical bending and electrical conductivity across different ratios of Arabic gum-graphite composite and copper. It also examines the potential differences among various electrode and dielectric materials in different self-powered sensor prototypes. Next, the chapter fully records the characterization of the sensor's signal, focusing on the voltage it produces. The results, including analyses of voltage as a function of force and distance, are thoroughly discussed. Additionally, durability tests on the self-powered sensor are conducted and will be explored further in this chapter. Finally, the chapter delves into applications involving human-machine interactions through IoT, including the development of a ping pong ball game that utilizes the sensor and WiFi.

4.2 Mechanical and Electrical Properties of Electrode

After completing the mechanical bending test, the results indicate that the Arabic gum-graphite composite weight ratio of 5:10 has Young's modulus of 0.26 GPa, 10:10 has Young's modulus of 0.32 GPa, 15:10 has Young's modulus of 0.45 GPa, and 20:10 has Young's modulus of 0.69 GPa, as indicated in Figure 4.1. In comparison, copper exhibits the highest Young's modulus of 130 GPa (Zhou et al., 2006). This data shows that copper is significantly stiffer than the Arabic gum-graphite composite samples, with the 5:10 ratio having the lowest stiffness. The findings suggest that as the weight ratio of Arabic gum increases, the material becomes stiffer, indicating reduced elasticity and requiring greater force to bend. Additionally, another study underscores the direct relationship between Young's modulus and stiffness in materials modified with Arabic gum, showing that as the Arabic gum content increases, the slope of the stress-strain curve steepens, further confirming the increase in stiffness (Brzyski, 2021). The optimum weight ratio chosen for the Arabic gum-graphite composite is 5:10 based on mechanical properties because it has the least Young's modulus among the other ratios.

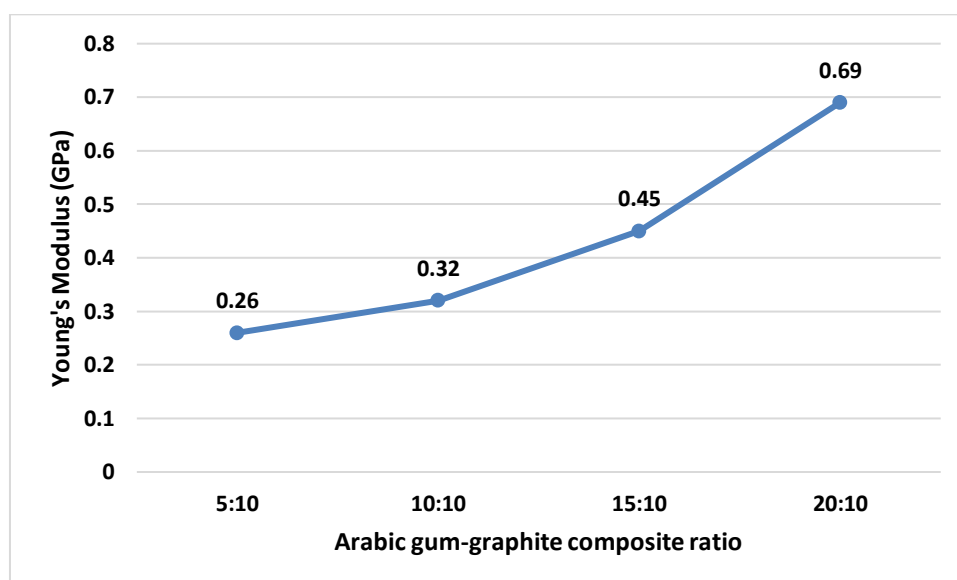


Figure 4.1: Young's Modulus of Arabic gum-graphite composite.

Next, the resistance measurements were recorded and subsequently converted into electrical conductivity values. The results indicate that copper exhibits the highest electrical conductivity, with a value of 227.273 (S/m). In comparison, the Arabic gum-graphite composites show varying degrees of conductivity: the 5:10 weight ratio has a conductivity of 10 (S/m), the 10:10 ratio has a conductivity of 1.667 (S/m), the 15:10 ratio measures at 0.833 (S/m), and the 20:10 ratio has the lowest conductivity of 0.556 (S/m), as shown through Figure 4.2. These findings highlight that the Arabic gum-graphite composite with a 20:10 weight ratio exhibits the lowest electrical conductivity, while copper maintains the highest. This difference in conductivity can be attributed to the graphite content within the composites; the 20:10 ratio has a significantly lower graphite content compared to the 5:10 ratio, which has a higher concentration of graphite. Since graphite is rich in carbon, an increase in its content directly enhances the material's electrical conductivity. Consequently, the higher the graphite content in the composite, the better its ability to conduct electricity. Thus, the optimum weight ratio chosen for the Arabic gum-graphite composite is 5:10 based on electrical properties because it has the highest electrical conductivity among the other ratios.

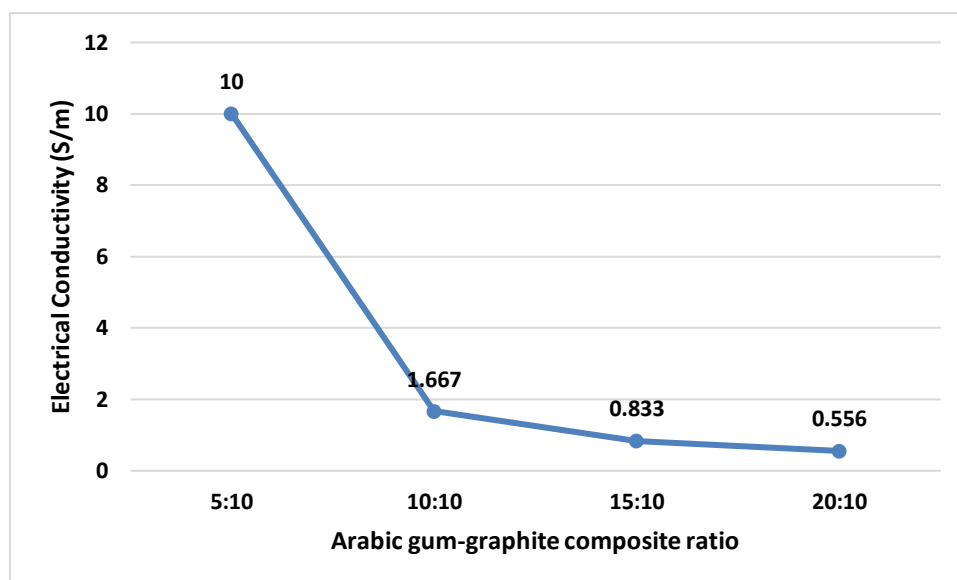


Figure 4.2: Electrical conductivity of Arabic gum-graphite composite.

Furthermore, the Scanning Electron Microscope (SEM) analysis provided a detailed and well-labeled image of the samples, with dimensions clearly marked for accurate measurement, as stated in Figure 4.3. The chosen sample materials—comprising a copper sheet and Arabic gum-graphite composite in a 5:10 weight ratio—were selected based on their high electrical conductivity. Upon magnification to 100x, the SEM image revealed numerous significant pores and several surface cracks on the Arabic gum-graphite composite, with the largest pore diameter measuring up to 114 μm . In contrast, the copper sheet displayed a smooth surface with minimal porosity and no visible cracks. The increased porosity and the presence of cracks in the Arabic gum-graphite composite contribute to its rougher surface texture and reduced stiffness. On the other hand, the copper sheet, with its minimal porosity and lack of surface defects, maintains a smoother surface and greater stiffness. This analysis highlights the correlation between surface roughness and porosity, demonstrating that as porosity increases, surface roughness and stiffness decrease, whereas materials with smoother surfaces, like copper, tend to exhibit greater stiffness and structural integrity. Therefore, the Arabic gum-graphite composite with a weight ratio of 5:10 was chosen due to its rougher surface compared to the copper sheet, which is expected to produce higher voltage.

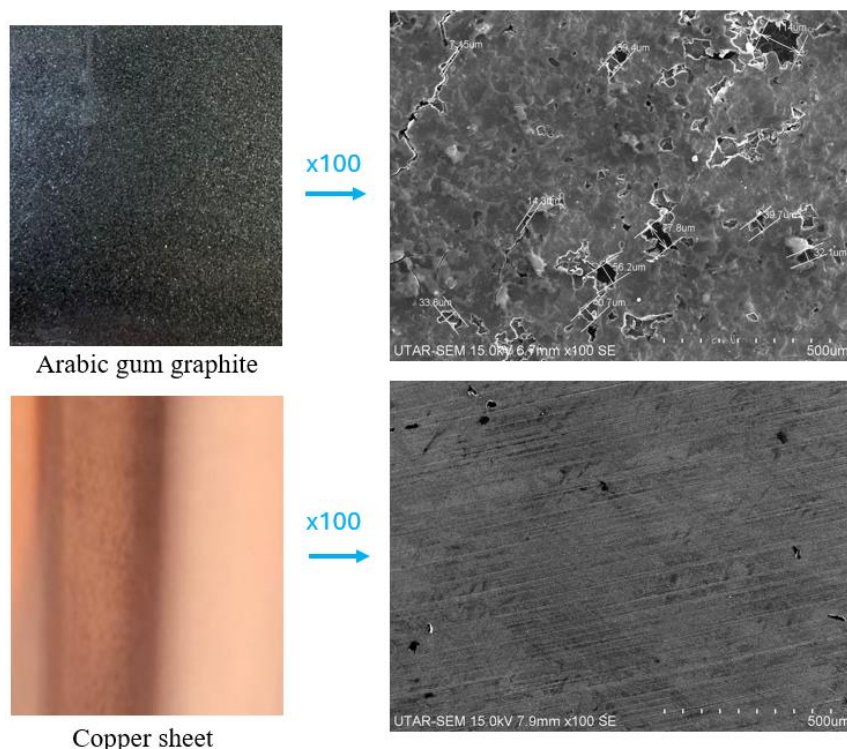


Figure 4.3: SEM of Arabic gum-graphite composite and copper.

4.3 Characterization of Green Self-powered Sensor

Figure 4.4 shows the complete fabrication process for prototypes of green, triboelectric, self-powered sensors. These include PVC/cloth-copper (see Figure 4.4 (1)), PVC/paper-copper (see Figure 4.4 (2)), and PVC/paper-Arabic gum-graphite composite (see Figure 4.4 (3)). Beneath the copper electrode, it has been observed that the potential difference generated between PVC and paper is 0.44V, which is higher than that between PVC and cloth at 0.22V. This difference can be attributed to the triboelectric series, in which paper is generally more triboelectrically positive than cloth, as it more readily loses electrons. Consequently, the paper has been selected for further testing with PVC under an Arabic gum-graphite composite electrode. The Arabic gum-graphite composite with a weight ratio of 5:10 exhibits the highest electrical conductivity, while the ratio of 20:10 shows the lowest. It was discovered that the weight ratio of 5:10 produces a potential difference of 1.4V, surpassing the 1.13V of the 20:10 ratio, as proven in Figure 4.5. This enhancement is due to the higher electrical conductivity, which minimizes energy losses, enables more efficient charge transport, and reduces the resistance affecting the electrical current flow. Additionally, the electrode made from Arabic gum-

graphite composite generates a higher potential difference than one made from copper. This advantage stems from the Arabic gum-graphite composite's porous and rough surface, which increases the effective contact area with the dielectric material, leading to more significant charge accumulation compared to smoother, less porous materials like copper. The flexibility of Arabic gum-graphite composite, attributed to its lesser stiffness, allows it to better conform to the contours of the opposing material during contact, thereby increasing the effective contact area and enhancing charge generation. Consequently, the optimal green material combination identified includes PVC as the negative dielectric material and paper as the positive dielectric material, utilizing an Arabic gum-graphite composite electrode with a 5:10 weight ratio for further characterization tests.

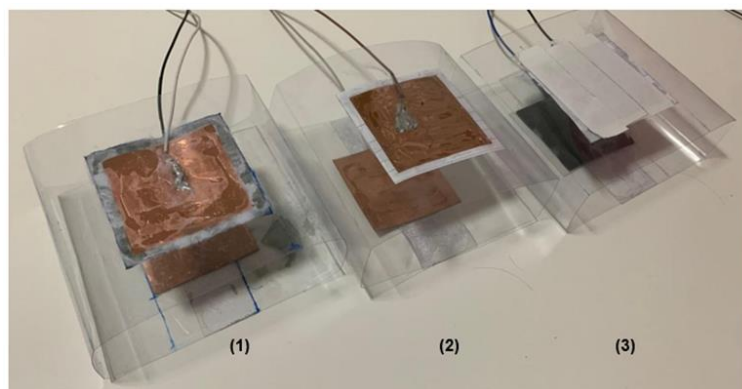


Figure 4.4: Prototype of self-powered sensors (1) PVC/cloth-copper, (2) PVC/paper-copper, and (3) PVC/paper-Arabic gum-graphite composite.

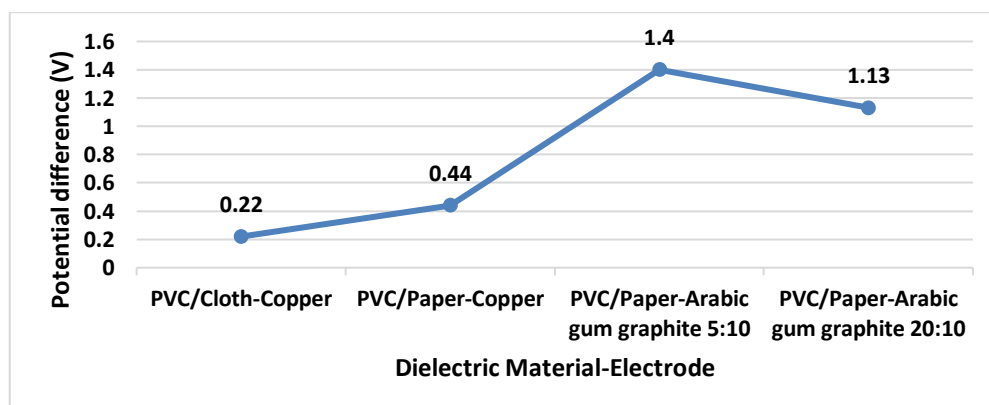


Figure 4.5: Potential differences are generated based on the types of materials used.

Initially, the behavior of the signal produced by a self-powered sensor is analyzed. The signal resulting from a single tap applying a force of 10N on the sensor is illustrated in Figure 4.6. When paper contacts the PVC surface, the latter becomes negatively charged, while the paper becomes positively charged. The Arabic gum-graphite composite, which interfaces with both materials, serves as an electrode to collect and retain these charges. As the materials are separated by the hand tap, the increasing distance between the charged surfaces of the paper and PVC alters the electric field, thereby generating a voltage. At the onset of separation, a peak in voltage occurs in one direction (negative). As separation progresses, the arrangement and balance of the remaining charges shift, frequently causing the voltage to reverse to the positive direction. This reversal happens as the diminishing influence of the opposing charges lessens, temporarily allowing the inherent charges on the Arabic gum-graphite composite electrodes to predominate. Ultimately, when the materials and their respective electrodes are completely separated and the system stabilizes, the charges either redistribute or dissipate into the environment, resulting in the voltage returning to zero. Figure 4.7 illustrates the working principle of the contact-separation mode in a triboelectric sensor.

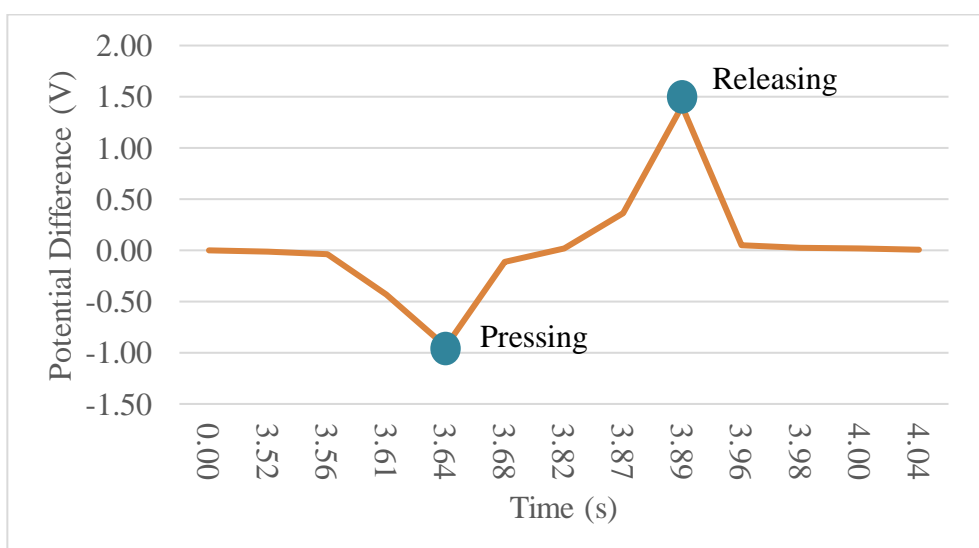


Figure 4.6: Sensor output from a single contact and separation event using PVC/Paper-Arabic gum-graphite (5:10).

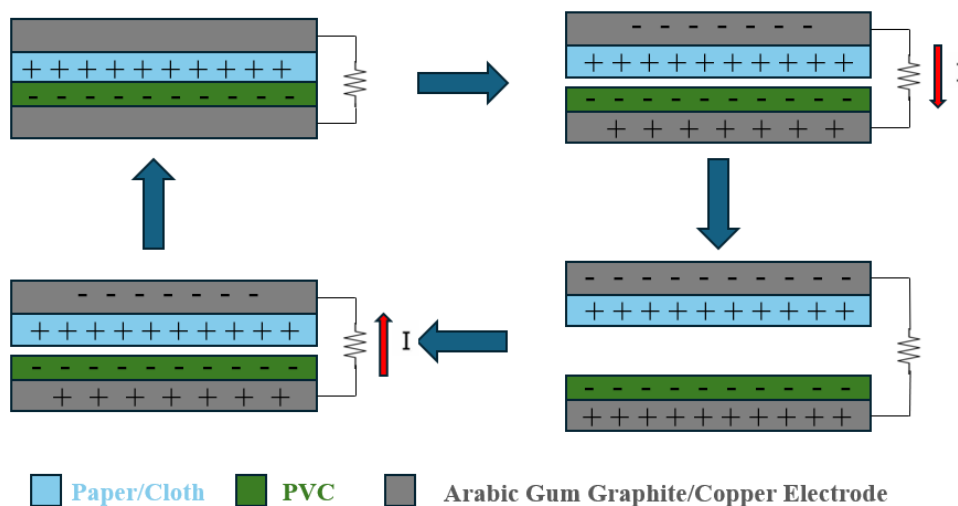


Figure 4.7: Working principle of contact separation mode.

The impact of the applied force on the potential difference is examined and the results are displayed in Figure 4.8. The graph indicates that as the applied force increases, so does the potential difference. This increase is attributed to the greater force pressing the surfaces more tightly together, minimizing the microscopic gaps between them. This close contact facilitates the accumulation of a higher density of charges at the interface. When these densely grouped charges separate, the intensified electrostatic forces generate a significantly higher voltage.

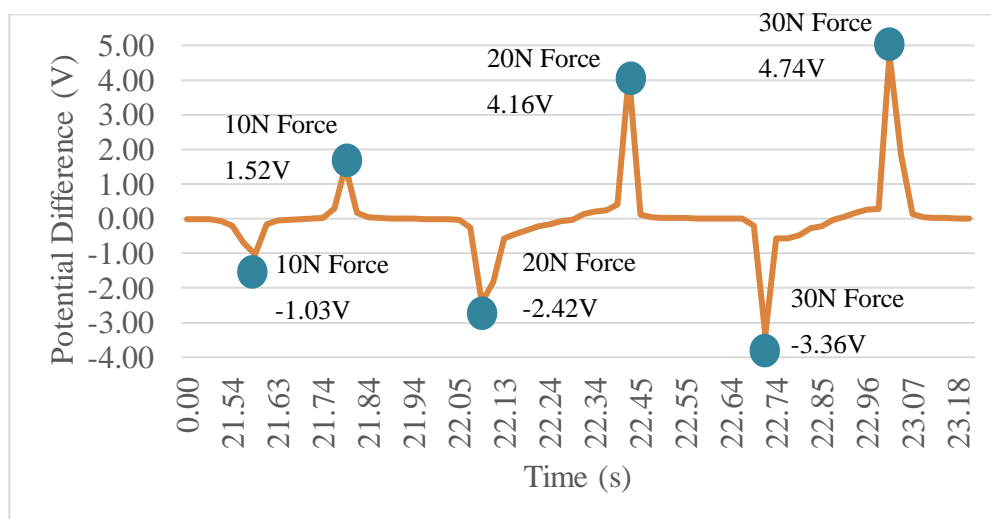


Figure 4.8: Output of the self-powered sensor with varying applied forces.

Additionally, the relationship between gap displacement and potential difference is analyzed and presented in Figure 4.9. The data in the graph demonstrate that the potential difference increases with larger gap displacement. This increase occurs because, in a triboelectric sensor, a larger gap displacement extends the electric field over a greater distance and reduces the capacitance. Consequently, the reduced capacitance leads to a higher voltage for the same amount of charge.

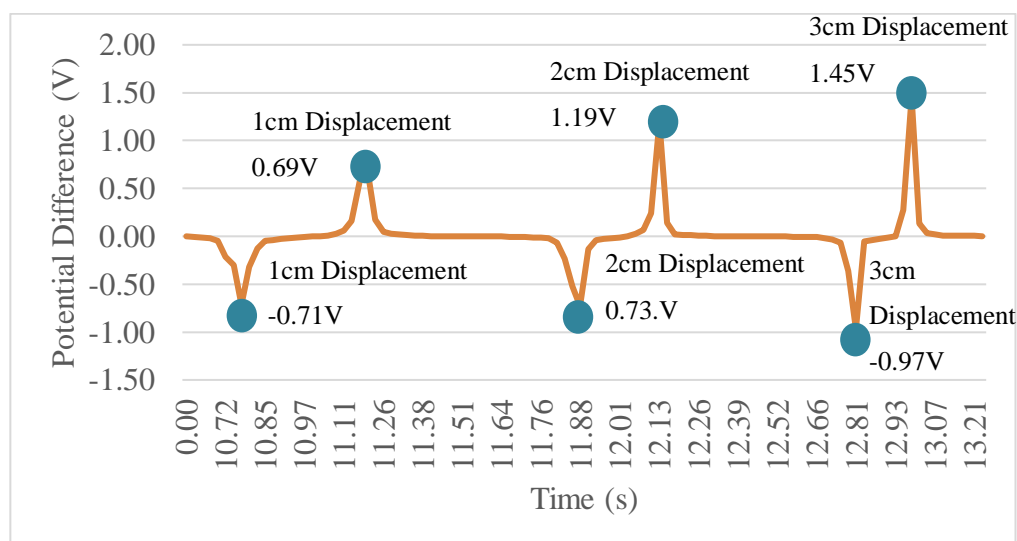


Figure 4.9: Output of the self-powered sensor with varying applied displacement.

4.4 Durability Test

Figure 4.10 displays the test output performance of PVC/paper-Arabic gum-graphite composite at a weight ratio of 5:10 over 1000 cycles based on an input frequency of 0.5Hz of machine tapping. The initial voltage generated is 1.44V, increasing to a final voltage of 1.75V. This gradual increase in voltage can be attributed to the accumulation of residual charges on the surfaces of the dielectric materials with each tap. The voltage output remains stable and does not degrade over 1000 cycles, indicating that this setup is well-suited for further application as a triboelectric sensor. Another durability test was conducted comparing PVC/paper and PVC/cloth, both utilizing copper electrodes and subjected to 1000 cycles of tapping, as shown in Appendix A Figure A-1 and Figure A-2. Both configurations demonstrated stable output throughout the 1000 cycles test, indicating robust performance and reliability

of the triboelectric sensor in various material combinations. The consistent voltage output across these different setups further supports the suitability of these materials for durable and efficient triboelectric sensing applications.

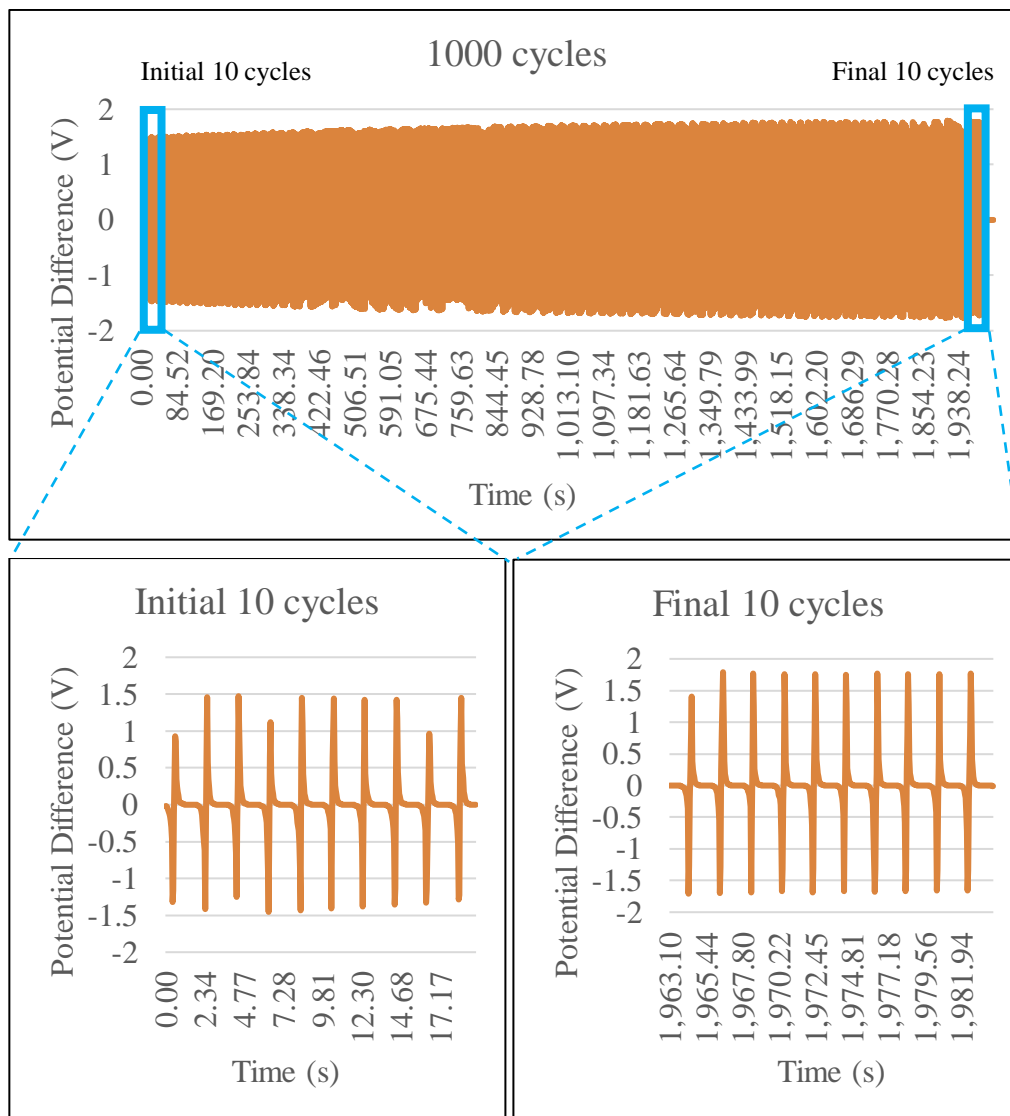


Figure 4.10: Output of PVC/paper-Arabic gum-graphite composite using self-powered sensor over 1000 cycles.

4.5 IOT Self-Powered Sensor Application

The ping pong game application, depicted in Figure 4.11, utilizes a self-powered sensor activated by hand tapping. This application captures the voltage produced by the sensor and processes the output accordingly. When a hand tap on the triboelectric sensor produces a voltage greater than the 3V threshold as seen in Figure 4.12, the system interprets this as input from the

user and adjusts the position of the ping-pong paddle accordingly. The direction in which the paddle moves depends on which sensor registers the input. If the sensor on the right is triggered, the paddle moves upward. Conversely, if the left sensor detects a voltage above the threshold, the paddle is moved downward. This allows for smooth and responsive gameplay, where the paddle dynamically adjusts based on real-time sensor feedback from the player's hand taps. This interaction mechanism provides a simple yet effective way to control the paddle in the ping pong game. The ping pong ball strikes the paddle and rebounds. If the ball subsequently hits the frame behind the paddle, points are awarded to either the computer or human player, depending on who last hit the ball.

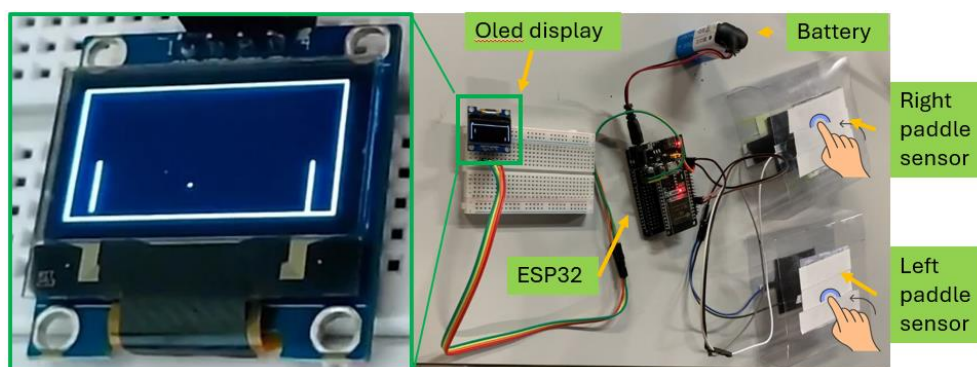


Figure 4.11: Ping pong game controlled by self-powered sensor.

```

right_state |= (right_voltage > TRIBO_THRESHOLD);
left_state |= (left_voltage > TRIBO_THRESHOLD);
if (right_state) {
  player_y -= 1;
}
if (left_state) {
  player_y += 1;
}

```

Figure 4.12: Ping pong game controlled by self-powered sensor.

Figure 4.13 illustrates the Blynk IoT dashboard displaying two scores, one for the computer player and one for the human player. These scores are transmitted wirelessly in real-time via WiFi, allowing them to be displayed on

a laptop or phone. Conceptually, this setup allows a doctor to monitor whether a patient has reached the targeted score without requiring a physical visit. If the score surpasses 9, the OLED display will show which player won the game, and the game will automatically restart.

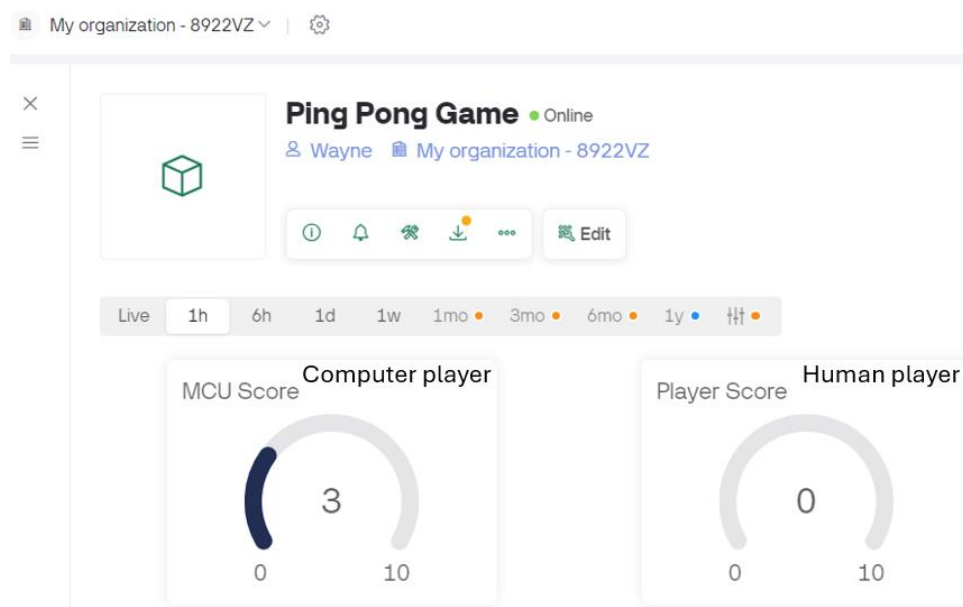


Figure 4.13: Blynk IOT dashboard with 2 scores.

4.6 Summary

In mechanical bending properties, the Arabic gum-graphite composite electrode with a 5:10 weight ratio exhibits the lowest Young's modulus. Electrically, it is more conductive than other weight ratios, though less so than copper, and its rougher surface compared to copper results in higher voltage output. Therefore, the 5:10 weight ratio is chosen as the optimal electrode composition. The optimal green material combination identified includes PVC as the negative dielectric and paper as the positive, using this Arabic gum-graphite composite electrode for further characterization tests. The greater the force applied to the sensor, the larger the potential difference generated; similarly, increased gap displacement results in greater potential difference. Although the Arduino setup only requires a voltage above 3V to trigger paddle movement, generating a higher voltage ensures consistent performance by providing a margin of reliability that accommodates variations in contact force or sensor fluctuations, thereby improving the responsiveness and stability of

the ping pong paddle control. Additionally, the sensor has been proven to function correctly over 1,000 tapping cycles. Subsequently, the sensor was used in a ping pong game to capture paddle movements left and right, with an IoT system transmitting score data via WiFi through Blynk.

CHAPTER 5

CONCLUSIONS AND RECOMMENDATIONS

5.1 Conclusions

At the project's conclusion, a green self-powered sensor was successfully designed and fabricated. Initial tests on its mechanical and electrical properties revealed that the Arabic gum-graphite composite electrode with a 5:10 weight ratio could replace copper, generating a higher potential difference. Paper, proving to be more positively triboelectric than cloth, was selected as the biodegradable material, while PVC was chosen for its reusability and effectiveness as a negative triboelectric material.

Characterization of the sensor has demonstrated its ability to generate a voltage ranging from approximately -1.68V to 1.75V. Additionally, the sensor's voltage increases with greater force and gap displacement during tapping. Repeatability tests over 1000 cycles have confirmed that the chosen green sensor material maintains consistent potential difference and provides stable output.

After characterization, a prototype was developed integrating a self-powered sensor into an IoT system for an interactive Ping Pong game on an ESP32 microcontroller with an OLED display, aimed at elderly rehabilitation. Players move the paddle by tapping the sensor, with performance scores transmitted in real time via Blynk over WiFi, enabling doctors to monitor patient progress remotely.

5.2 Recommendations for Future Work

The sensor design that has been proposed and developed could benefit from several enhancements. One key improvement involves replacing the flat arch structure cover, which currently uses a PVC sheet as a flexible spacer, with a sponge. The motivation behind this change is to address the issue of plastic deformation. Specifically, if the PVC spacer is accidentally folded to a certain degree during tapping, it can leave a permanent mark or crease line, which subsequently reduces the material's ability to separate back effectively. In

contrast, a cellulose sponge would offer enhanced flexibility and better maintain its form, making it a more suitable, biodegradable, and reusable material for this application.

Additionally, the current model of the green self-powered sensor is not waterproof, which poses limitations for its use in various environments. The core material, Arabic gum-graphite composite, is rewettable and can be deformed into any shape, which is a useful feature but also makes the sensor vulnerable to water damage. To overcome this, it is advisable to design the sensor with a waterproof cover case. This enhancement would protect the internal components from moisture and expand the sensor's applicability to more diverse and potentially wet conditions, thereby increasing its durability and functionality.

These proposed changes aim not only to improve the sensor's structural integrity and flexibility but also to enhance its usability and longevity in practical applications. By addressing these issues, the sensor can be made more robust and versatile, paving the way for broader deployment in real-world settings.

REFERENCES

- Abbott, T., 2009. Why choose magnesium? *Materials Science Forum*, 618-619, pp.3-6. <https://doi.org/10.4028/www.scientific.net/MSF.618-619.3>.
- Brzyski, P., 2021. The influence of gum arabic admixture on the mechanical properties of lime-metakaolin paste used as binder in hemp concrete. *Materials*, 14(22). <https://doi.org/10.3390/ma14226775>.
- Bukhari, M.U., Naqvi, S.R., Nizamuddin, S., Siddiqui, M.T.H., Younis, M., Zaidi, S.J. and Mubarak, N.M., 2022. Waste to energy: Facile, low-cost and environment-friendly triboelectric nanogenerators using recycled plastic and electronic wastes for self-powered portable electronics. *Energy Reports*, 8, pp.1687–1695. <https://doi.org/10.1016/j.egy.2021.12.072>.
- Dangelico, R.M. and Pontrandolfo, P., 2010. From green product definitions and classifications to the Green Option Matrix. *Journal of Cleaner Production*, 18(16–17), pp.1608–1628. <https://doi.org/10.1016/j.jclepro.2010.07.007>.
- Farzin, M.A., Naghib, S.M. and Rabiee, N., 2024. Advancements in bio-inspired self-powered wireless sensors: Materials, mechanisms, and biomedical applications. *ACS Biomaterials Science and Engineering*, pp.1262–1301. <https://doi.org/10.1021/acsbmaterials.3c01633>.
- Guo, H., Yeh, M.-H., Lai, Y.-C., Zi, Y., Wu, C., Wen, Z., Hu, C. and Wang, Z.L., 2016. A water-proof triboelectric-electromagnetic hybrid generator for energy harvesting in harsh environments. *Advanced Energy Materials*, 6(6). <https://doi.org/10.1002/aenm.201501593>.
- Hao, D., Li, X., Liu, D. and Zhang, Y., 2022. Solar energy harvesting technologies for PV self-powered applications: A comprehensive review. *Renewable Energy*, pp.678–697. <https://doi.org/10.1016/j.renene.2022.02.066>.
- Kurra, N. and Kulkarni, G.U., 2013. Pencil-on-paper: Electronic devices. *Lab on a Chip*, 13(15), pp.2866–2873. <https://doi.org/10.1039/c3lc50406a>.
- Lai, Z., Wang, J., He, Y., Dong, J. and Wang, Z., 2022. Self-powered and self-sensing devices based on human motion. *Joule*, pp.1501–1565. <https://doi.org/10.1016/j.joule.2022.06.013>.
- Li, J., Liu, H., Yuan, S. and Zhang, Y., 2023. Self-powered droplet sensor based on triboelectric nanogenerator toward the Internet-of-Things (IoT) alarm system. *ACS Applied Electronic Materials*, 5(11), pp.6026–6036. <https://doi.org/10.1021/acsaelm.3c01018>.
- Liu, S., Zhang, W., Xu, Q. and Li, H., 2023. Flexible, durable, green thermoelectric composite fabrics for textile-based wearable energy harvesting and self-powered sensing. *Composites Science and Technology*, 243. <https://doi.org/10.1016/j.compscitech.2023.110245>.

Pagett, M., Kornecki, L., Ivanov, D. and Eckert, J., 2023. Reusing waste coffee grounds as electrode materials: Recent advances and future opportunities. *Global Challenges*. <https://doi.org/10.1002/gch2.202200093>.

Pan, R., Gao, S., Zhang, Y., Li, S. and Hu, Z., 2018. Fully biodegradable triboelectric nanogenerators based on electrospun polylactic acid and nanostructured gelatin films. *Nano Energy*, 45, pp.193–202. <https://doi.org/10.1016/j.nanoen.2017.12.048>.

Peppler, K., Salen Tekinbaş, K., Gresalfi, M. and Santo, R., 2019. Squishing circuits: Circuitry learning with electronics and playdough in early childhood. *Journal of Science Education and Technology*, 28(2), pp.118–132. <https://doi.org/10.1007/s10956-018-9752-2>.

Preparation of graphite conductive paint and its application to the construction of RC circuits on paper, 2016. *Physics Education*, 51(5). <http://iopscience.iop.org/0031-9120/51/5/055011>.

Rahmani, H., Shahbazi, M.A., Hajizadeh, Z. and Vashae, D., 2023. Next-generation IoT devices: Sustainable eco-friendly manufacturing, energy harvesting, and wireless connectivity. *IEEE Journal of Microwaves*, 3(1), pp.237–255. <https://doi.org/10.1109/JMW.2022.3228683>.

Saravanakumar, B., Mohapatra, P., Roy, A., Ray, S.S. and Kim, S.-J., 2015. Fabrication of an eco-friendly composite nanogenerator for self-powered photosensor applications. *Carbon*, 84(C), pp.56–65. <https://doi.org/10.1016/j.carbon.2014.11.041>.

Sojan, S. and Kulkarni, R.K., 2016. A comprehensive review of energy harvesting techniques and its potential applications. *International Journal of Computer Applications*. https://www.researchgate.net/publication/301335724_A_Comprehensive_Review_of_Energy_Harvesting_Techniques_and_its_Potential_Applications.

Syeda Adila, A., Husam, A. and Husi, G., 2018. Towards the self-powered Internet of Things (IoT) by energy harvesting: Trends and technologies for green IoT. <https://ieeexplore.ieee.org/document/8355305>.

Xu, Z., Chang, Y. and Zhu, Z., 2024. A triboelectric nanogenerator based on bamboo leaf for biomechanical energy harvesting and self-powered touch sensing. *Electronics* (Switzerland), 13(4). <https://doi.org/10.3390/electronics13040766>.

Zhou, Z.M., Zhou, Z., Wang, Z., Wu, Y. and Wang, G., 2006. The evaluation of Young's modulus and residual stress of copper films by microbridge testing. *Sensors and Actuators, A: Physical*, 127(2), pp.392–397. <https://doi.org/10.1016/j.sna.2005.12.036>.

APPENDICES

Appendix A: Supporting Graphs for the Durability Test

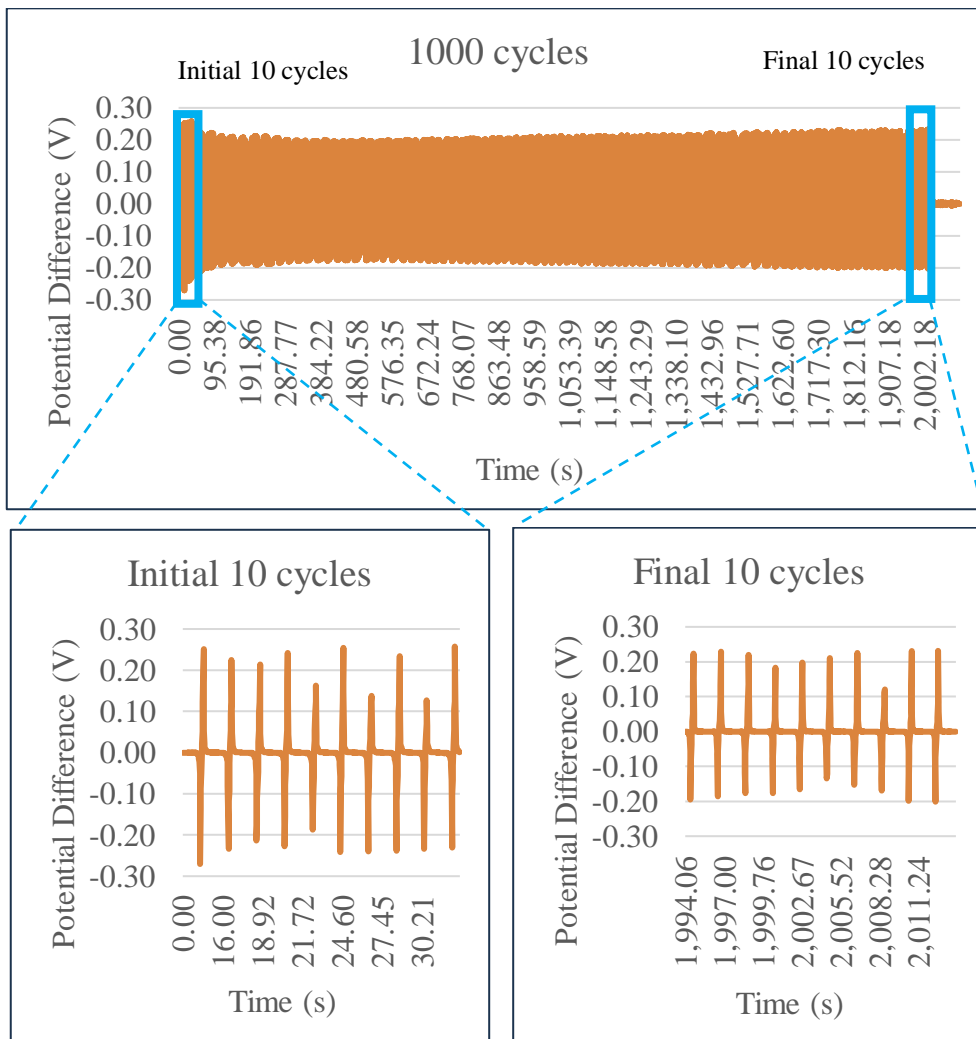


Figure A-1: Output of PVC/Cloth-Copper sensor over 1000 cycles.

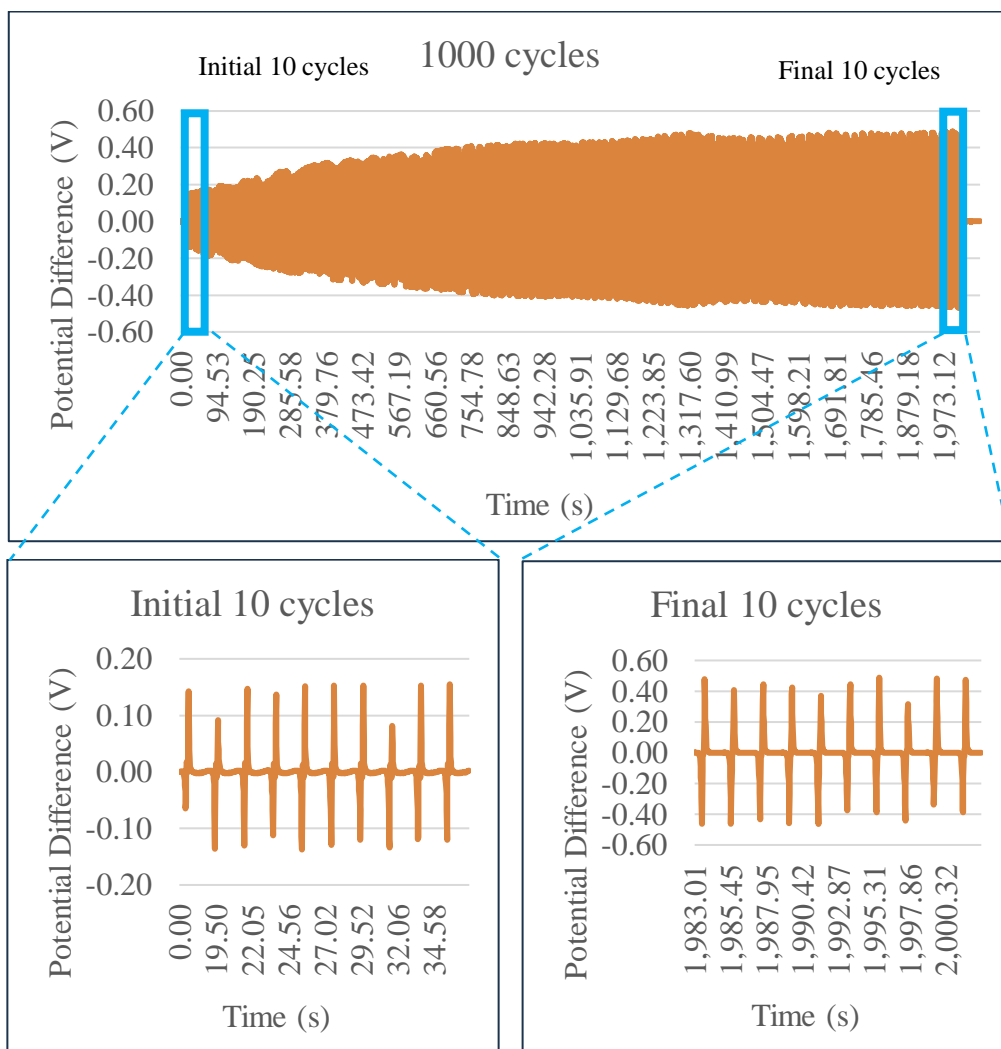


Figure A-2: Output of PVC/Paper-Copper sensor over 1000 cycles.

Appendix B: Supporting Attachments for Ping Pong Ball Application

Code for Ping Pong Ball Application:

```

#define BLYNK_PRINT Serial

/* Fill in information from Blynk Device Info here */
#define BLYNK_TEMPLATE_ID "TMPL62bZe33Gr"
#define BLYNK_TEMPLATE_NAME "Ping Pong Game"
#define BLYNK_AUTH_TOKEN "P6ZjovAdbtSe7ep9UC83n3CdXNruZ-2Q"

#include <WiFi.h>
#include <WiFiClient.h>
#include <BlynkSimpleEsp32.h>
#include <Adafruit_GFX.h>
#include <Adafruit_SSD1306.h>

// WiFi credentials
char ssid[] = "TY";
char pass[] = "teckyuan19";

// Triboelectric sensor pins
#define RIGHT_BUTTON_PIN 34 // Pin for "right" button
#define LEFT_BUTTON_PIN 35 // Pin for "left" button

const unsigned long PADDLE_RATE = 32;
const unsigned long BALL_RATE = 8;
const uint8_t PADDLE_HEIGHT = 12;
const uint8_t SCORE_LIMIT = 10;
const float TRIBO_THRESHOLD = 3.0; // Voltage threshold for tribo sensor

Adafruit_SSD1306 display = Adafruit_SSD1306(128, 64, &Wire, -1);

bool game_over, win;
uint8_t player_score, mcu_score;
uint8_t ball_x = 53, ball_y = 26;
uint8_t ball_dir_x = 1, ball_dir_y = 1;

unsigned long ball_update;
unsigned long paddle_update;

const uint8_t MCU_X = 12;
uint8_t mcu_y = 16;

const uint8_t PLAYER_X = 115;
uint8_t player_y = 16;

void setup() {

```

```

Serial.begin(9600);

// Initialize WiFi and Blynk connection
WiFi.begin(ssid, pass);
while (WiFi.status() != WL_CONNECTED) {
  delay(500);
  Serial.print(".");
}
Serial.println("");
Serial.println("WiFi connected");

Blynk.begin(BLYNK_AUTH_TOKEN, ssid, pass);

display.begin(SSD1306_SWITCHCAPVCC, 0x3C);
display.display();
unsigned long start = millis();

display.clearDisplay();
drawCourt();

while (millis() - start < 2000);

display.display();

ball_update = millis();
paddle_update = ball_update;
}

void loop() {
  Blynk.run();

  bool update_needed = false;
  unsigned long time = millis();

  static bool right_state = false;
  static bool left_state = false;

  int right_value = analogRead(RIGHT_BUTTON_PIN);
  float right_voltage = right_value * (3.3 / 4095.0); // ESP32 ADC conversion

  int left_value = analogRead(LEFT_BUTTON_PIN);
  float left_voltage = left_value * (3.3 / 4095.0); // ESP32 ADC conversion

  Serial.print(right_voltage);
  Serial.print(",");
  Serial.println(left_voltage);

  right_state |= (right_voltage > TRIBO_THRESHOLD);
  left_state |= (left_voltage > TRIBO_THRESHOLD);

```

```

if (time > ball_update) {
    uint8_t new_x = ball_x + ball_dir_x;
    uint8_t new_y = ball_y + ball_dir_y;

    if (new_x == 0 || new_x == 127) {
        ball_dir_x = -ball_dir_x;
        new_x += ball_dir_x + ball_dir_x;

        if (new_x < 64) {
            player_score++;
        } else {
            mcu_score++;
        }
    }

    if (player_score == SCORE_LIMIT || mcu_score == SCORE_LIMIT) {
        win = player_score > mcu_score;
        game_over = true;
    }
}

if (new_y == 0 || new_y == 53) {
    ball_dir_y = -ball_dir_y;
    new_y += ball_dir_y + ball_dir_y;
}

if (new_x == MCU_X && new_y >= mcu_y && new_y <= mcu_y + PADDLE_HEIGHT) {
    ball_dir_x = -ball_dir_x;
    new_x += ball_dir_x + ball_dir_x;
}

if (new_x == PLAYER_X && new_y >= player_y && new_y <= player_y + PADDLE_HEIGHT) {
    ball_dir_x = -ball_dir_x;
    new_x += ball_dir_x + ball_dir_x;
}

display.drawPixel(ball_x, ball_y, BLACK);
display.drawPixel(new_x, new_y, WHITE);
ball_x = new_x;
ball_y = new_y;

ball_update += BALL_RATE;

update_needed = true;
}

if (time > paddle_update) {
    paddle_update += PADDLE_RATE;

    display.drawFastVLine(MCU_X, mcu_y, PADDLE_HEIGHT, BLACK);
    const uint8_t half_paddle = PADDLE_HEIGHT >> 1;

```

```
if (mcu_y + half_paddle > ball_y) {
    int8_t dir = ball_x > MCU_X ? -1 : 1;
    mcu_y += dir;
}

if (mcu_y + half_paddle < ball_y) {
    int8_t dir = ball_x > MCU_X ? 1 : -1;
    mcu_y += dir;
}

if (mcu_y < 1) {
    mcu_y = 1;
}

if (mcu_y + PADDLE_HEIGHT > 53) {
    mcu_y = 53 - PADDLE_HEIGHT;
}

display.drawFastVLine(MCU_X, mcu_y, PADDLE_HEIGHT, WHITE);
display.drawFastVLine(PLAYER_X, player_y, PADDLE_HEIGHT, BLACK);

if (right_state) {
    player_y -= 1;
}

if (left_state) {
    player_y += 1;
}

right_state = left_state = false;

if (player_y < 1) {
    player_y = 1;
}

if (player_y + PADDLE_HEIGHT > 53) {
    player_y = 53 - PADDLE_HEIGHT;
}

display.drawFastVLine(PLAYER_X, player_y, PADDLE_HEIGHT, WHITE);

update_needed = true;
}

if (update_needed) {
    if (game_over) {
        const char* text = win ? "YOU WIN!!" : "YOU LOSE!";
        display.clearDisplay();
        display.setCursor(40, 28);
    }
}
```

```
display.print(text);
display.display();

delay(5000);

display.clearDisplay();
ball_x = 53;
ball_y = 26;
ball_dir_x = 1;
ball_dir_y = 1;
mcu_y = 16;
player_y = 16;
mcu_score = 0;
player_score = 0;
game_over = false;
drawCourt();
}

display.setTextColor(WHITE, BLACK);
display.setCursor(0, 56);
display.print(mcu_score);
display.setCursor(122, 56);
display.print(player_score);
display.display();

// Send the scores to Blynk
Blynk.virtualWrite(V2, mcu_score); // MCU score
Blynk.virtualWrite(V3, player_score); // Player score
}
}

void drawCourt() {
  display.drawRect(0, 0, 128, 54, WHITE);
}
```

Appendix C: Open Access to Image Rights

The screenshot shows the RightsLink interface for an article titled "Solar energy harvesting technologies for PV self-powered applications: A comprehensive review". The article is published in "Renewable Energy" by Elsevier in April 2022. The authors listed are Daning Hao, Lingfei Qi, Alaeldin M. Tairab, Ammar Ahmed, Ali Azam, Dabing Luo, Yajia Pan, Zutao Zhang, and Jinyue Yan. The interface includes a "Creative Commons Attribution-NonCommercial-No Derivatives License (CC BY NC ND)" section, which states that the article is published under these terms and provides instructions on how to use the article for non-commercial purposes. There are "BACK" and "CLOSE WINDOW" buttons at the bottom of the license section. At the very bottom of the page, there is a copyright notice for 2024 and links to various policies.

Figure C- 1: Principle of PV self-powered technologies.

9/12/24, 3:39 PM RightsLink Printable License


**JOHN WILEY AND SONS LICENSE
TERMS AND CONDITIONS**


Sep 12, 2024

This Agreement between Wayne Lim Yin Hern ("You") and John Wiley and Sons ("John Wiley and Sons") consists of your license details and the terms and conditions provided by John Wiley and Sons and Copyright Clearance Center.

License Number	5866370361036
License date	Sep 12, 2024
Licensed Content Publisher	John Wiley and Sons
Licensed Content Publication	Advanced Energy Materials
Licensed Content Title	A Water-Proof Triboelectric-Electromagnetic Hybrid Generator for Energy Harvesting in Harsh Environments
Licensed Content Author	Hengyu Guo, Zhen Wen, Yunlong Zi, et al
Licensed Content Date	Dec 23, 2015
Licensed Content Volume	6
Licensed Content Issue	6
Licensed Content Pages	7
Type of use	Dissertation/Thesis
Requestor type	University/Academic
Format	Electronic

Figure C- 2: Practical of the water-proof hybrid generator for harvesting water-flow energy in the water.


WL © 🔍

Advancements in Bio-inspired Self-Powered Wireless Sensors: Materials, Mechanisms, and Biomedical Applications

 Author: Mohammad Ali Farzin, Seyed Morteza Naghib, Navid Rabiee
 Publication: ACS Biomaterials Science & Engineering
 Publisher: American Chemical Society
 Date: Mar 1, 2024
Copyright © 2024, American Chemical Society

PERMISSION/LICENSE IS GRANTED FOR YOUR ORDER AT NO CHARGE
 This type of permission/license, instead of the standard Terms and Conditions, is sent to you because no fee is being charged for your order. Please note the following:

- Permission is granted for your request in both print and electronic formats, and translations.
- If figures and/or tables were requested, they may be adapted or used in part.
- Please print this page for your records and send a copy of it to your publisher/graduate school.
- Appropriate credit for the requested material should be given as follows: "Reprinted (adapted) with permission from (COMPLETE REFERENCE CITATION). Copyright (YEAR) American Chemical Society." Insert appropriate information in place of the capitalized words.
- One-time permission is granted only for the use specified in your RightsLink request. No additional uses are granted (such as derivative works or other editions). For any uses, please submit a new request.

If credit is given to another source for the material you requested from RightsLink, permission must be obtained from that source.

BACK
CLOSE WINDOW

Figure C- 3: Anode and cathode pastes that are completely edible are contained inside a hollow almond to form an implantable ethanol biofuel cell.

Journals & Magazines > IEEE Journal of Microwaves > Volume: 3 Issue: 1 ?

Next-Generation IoT Devices: Sustainable Eco-Friendly Manufacturing, Energy Harvesting, and Wireless Connectivity

Publisher: IEEE Cite This PDF

Hamed Rahmani  ; Darshan Shetty  ; Mahmoud Wagih  ; Yasaman Ghasempour  ; Valentina Palazzi  ; Nuno B. C... All Authors

35
Cites in
Papers

7576
Full
Text Views







 Open Access
Under a Creative Commons License

Figure C- 4: (a) Matching network with 50Ω antenna and (b) matched single-ended loop antenna.

9/12/24, 7:49 PM

RightsLink Printable License

ELSEVIER LICENSE
TERMS AND CONDITIONS

Sep 12, 2024

This Agreement between Wayne Lim Yin Hern ("You") and Elsevier ("Elsevier") consists of your license details and the terms and conditions provided by Elsevier and Copyright Clearance Center.

License Number	5866470246969
License date	Sep 12, 2024
Licensed Content Publisher	Elsevier
Licensed Content Publication	Composites Science and Technology
Licensed Content Title	Flexible, durable, green thermoelectric composite fabrics for textile-based wearable energy harvesting and self-powered sensing
Licensed Content Author	Siqi Liu, Mingxia Zhang, Junhua Kong, Hui Li, Chaobin He
Licensed Content Date	Oct 20, 2023
Licensed Content Volume	243
Licensed Content Issue	n/a
Licensed Content Pages	1
Start Page	110245
End Page	0
Type of Use	reuse in a thesis/dissertation

Figure C- 5: Design of CNT/PLA TE composite fabric and its function in wearable TE generators and temperature sensing.

9/12/24, 7:56 PM

RightsLink Printable License

ELSEVIER LICENSE
TERMS AND CONDITIONS

Sep 12, 2024

This Agreement between Wayne Lim Yin Hern ("You") and Elsevier ("Elsevier") consists of your license details and the terms and conditions provided by Elsevier and Copyright Clearance Center.

License Number	5866470711667
License date	Sep 12, 2024
Licensed Content Publisher	Elsevier
Licensed Content Publication	Carbon
Licensed Content Title	Fabrication of an eco-friendly composite nanogenerator for self-powered photosensor applications
Licensed Content Author	Balasubramaniam Saravanakumar, Kaliannan Thiagarajan, Nagamalleswara Rao Alluri, Shin SoYoon, Kim Taehyun, Zong-Hong Lin, Sang-Jae Kim
Licensed Content Date	Apr 1, 2015
Licensed Content Volume	84
Licensed Content Issue	n/a
Licensed Content Pages	10
Start Page	56
End Page	65
Type of Use	reuse in a thesis/dissertation

Figure C- 6: Digital image of the foot stamp at different stages.

9/12/24, 8:06 PM

RightsLink Printable License

ELSEVIER LICENSE
TERMS AND CONDITIONS

Sep 12, 2024

This Agreement between Wayne Lim Yin Hern ("You") and Elsevier ("Elsevier") consists of your license details and the terms and conditions provided by Elsevier and Copyright Clearance Center.

License Number	5866471291070
License date	Sep 12, 2024
Licensed Content Publisher	Elsevier
Licensed Content Publication	Joule
Licensed Content Title	Self-powered and self-sensing devices based on human motion
Licensed Content Author	Zhihui Lai, Junchen Xu, Chris R. Bowen, Shengxi Zhou
Licensed Content Date	Jul 20, 2022
Licensed Content Volume	6
Licensed Content Issue	7
Licensed Content Pages	65
Start Page	1501
End Page	1565
Type of Use	reuse in a thesis/dissertation

Figure C- 7: (a) Vertical contact separation mode, (b) sliding mode, (c) single electrode mode, and (d) free-standing mode. / Empirical Triboelectric Series.

ELSEVIER LICENSE
TERMS AND CONDITIONS

Sep 12, 2024

This Agreement between Wayne Lim Yin Hern ("You") and Elsevier ("Elsevier") consists of your license details and the terms and conditions provided by Elsevier and Copyright Clearance Center.

License Number	5866480116178
License date	Sep 12, 2024
Licensed Content Publisher	Elsevier
Licensed Content Publication	Nano Energy
Licensed Content Title	Fully biodegradable triboelectric nanogenerators based on electrospun polylactic acid and nanostructured gelatin films
Licensed Content Author	Ruizheng Pan, Weipeng Xuan, Jinkai Chen, Shurong Dong, Hao Jin, Xiaozhi Wang, Honglang Li, Jikui Luo
Licensed Content Date	Mar 1, 2018
Licensed Content Volume	45
Licensed Content Issue	n/a
Licensed Content Pages	10
Start Page	193
End Page	202
Type of Use	reuse in a thesis/dissertation

Figure C- 8: Production method of PLA and gelatin plates. / Photos of the disintegrating PLA/Mg sheets, Mg foil, and gelatine/Mg in natural water.

© 2024 by the authors. Licensee MDPI, Basel, Switzerland. This article is an open access article distributed under the terms and conditions of the Creative Commons Attribution (CC BY) license (<https://creativecommons.org/licenses/by/4.0/>).

Figure C- 9: Fabrication process of bamboo leaf and polytetrafluoroethylene (PTFE) film.


SPRINGER NATURE LICENSE
TERMS AND CONDITIONS

Sep 12, 2024

This Agreement between Wayne Lim Yin Hern ("You") and Springer Nature ("Springer Nature") consists of your license details and the terms and conditions provided by Springer Nature and Copyright Clearance Center.

License Number	5866490326326
License date	Sep 12, 2024
Licensed Content Publisher	Springer Nature
Licensed Content Publication	Journal of Science Education and Technology (Plenum)
Licensed Content Title	Squishing Circuits: Circuitry Learning with Electronics and Playdough in Early Childhood
Licensed Content Author	Kylie Pepler et al
Licensed Content Date	Oct 15, 2018
Type of Use	Thesis/Dissertation
Requestor type	academic/university or research institute
Format	electronic
Portion	figures/tables/illustrations
Number of figures/tables/illustrations	1
Will you be translating?	no

Figure C- 10: Simple circuit conductive dough with LED.



Reusing Waste Coffee Grounds as Electrode Materials: Recent Advances and Future Opportunities

Author: Wei Zhang, Geraint Sullivan, Kar Seng Teng, et al

Publication: Global Challenges

Publisher: John Wiley and Sons

Date: Oct 21, 2022

© 2022 The Authors. Global Challenges published by Wiley-VCH GmbH

Open Access Article

This is an open access article distributed under the terms of the [Creative Commons CC BY](#) license, which permits unrestricted use, distribution, and reproduction in any medium, provided the original work is properly cited.

You are not required to obtain permission to reuse this article.

For an understanding of what is meant by the terms of the Creative Commons License, please refer to [Wiley's Open Access Terms and Conditions](#).

Permission is not required for this type of reuse.

Wiley offers a professional reprint service for high quality reproduction of articles from over 1400 scientific and medical journals. Wiley's reprint service offers:

- Peer reviewed research or reviews
- Tailored collections of articles
- A professional high quality finish
- Glossy journal style color covers
- Company or brand customisation
- Language translations
- Prompt turnaround times and delivery directly to your office, warehouse or congress.

Please contact our Reprints department for a quotation. Email corporatesales@wiley.com or corporatesalesusa@wiley.com or corporatesalesDE@wiley.com.

Figure C- 11: Fabrication for WCG-derived TENG.